Sorting, trafficking and turnover of pH-regulatory transport protein NBCn1 (SLC4A7) in epithelial cells

Master's thesis by
Ida Axholm

Suporvisors:
Henning F. Bjerregaard
&
Stine F. Pedersen

June 1, 2018

Preface

The work presented in this Master's thesis was conducted from September 2017 to May 2018 in Professor Stine F. Pedersen's group NHE1, Department of Biology, Section for cell and developmental biology, University of Copenhagen. Internal supervisor: Henning F. Bjerregaard, Department of Science and Environment, Roskilde University.

Acknowledgements

First, I want to give my great thanks to my external supervisor, Professor Stine Falsig Pedersen for giving me the opportunity to work in the NHE1 group. It has been a pleasure to be a part of your team and your passion for science is a true inspiration.

I am greatful to the entire NHE1 group for creating a scientific environment with many laughs and great support. Many thanks to Marc Severin for great collaboration and inspiring discussions. Your scientific curiosity and love for biology have inspired me immensely. Many thanks to Julie Schnipper for introducing me to the NHE1 group. Your joyful spirit and admirable work ethics have been a gift to the entire group. Many thanks to technician Katrine Franklin Mark for her positive and caring being. Your systematic arrangements are curcial for the exchange of knowledge between the group members and save hours of work. Thank you!

I would like to express my graditude to Dan Ploug Christensen for his unrelenting willingness to help and his encouragement when things were less fun.

Thank you to all on the 5th floor for such a good time!

Abstract

Normal function of all epithelia relies on the correct polarized localization of ion transport proteins, and malfunctions in the trafficking of these proteins to the plasma membrane contribute to numerous diseases. Na^+, HCO_3^- cotransporter NBCn1 (SLC4A7) is a major regulator of pH_i in most cell types with important functions in the cardiovascular system, the kidneys, and other organ systems. The dysfunction of NBCn1 is implicated in several diseases, includig hypertension and cancer. In particular, NBCn1 plays a central role in breast cancer. Despite the importance of NBCn1 in physiology and disease, very little is known about the regulation and roles of NBCn1. Specifically, there is a near-complete lack of knowledge regarding NBCn1 biosynthesis, trafficking, and degradation pathways. Prior to this study, our lab performed mass spectrometry analysis of interaction partners of, revealing several putative C-tail interactions candidates. In this study, we performed co-IP to validate these suggested interactions partners. We found that NBCn1 interacts with γ-adaptin, suggesting NBCn1 sorting to the membrane via AP-1 clathrin-coated vesicles. Morover, we foung that NBCn1 interacts with lateral polaity proteins LLGL-1 and DLG, suggesting a lateral targeting pattern for NBCb1. Lastly, we found that scaffold protein RACK1 interacts with NBCn1 and that the proximal 22 amino acids of the C-tail are sufficient for RACK1 interaction.

Abbreviations

AE1	Anion Exchanger 1
AGT	O^6-alkylguanine-DNA alkyltransferase
AP	Adaptor Protein
BG	O^6-benzylguanine
BSA	Bovine Serum Albumin
BSE	Basolateral Sorting Endosomes
CA	Carbonic Anhydrase
Co-IP	Co-immunoprecipitation
DLG	Discs Large Homolog
DTT	Dithiothreitol
ER	Endoplasmic Reticulum
EPS15	EGFR Pathway Substrate 15
FBS	Fetal Bovine Serum
FCHO	FCH domain only
h	hour(s)
HEK293	Human Embryonic Kidney 293
IF	Immunofluorescence
IRBIT	IP_3 receptor binding protein released with inositol 1,4,5- triphosphate
KD	Knock-down
KO	Kock-out
LAMP-1	Lysosomal-Associated Membrane Protein 1
LE	Late Endosomes
LDS	Lithium Dodecyl Sulfate
MDCK-II	Madin Darby Canine Kidney II
NBCn1	Electroneutral Na^+, HCO_3^- Cotransporter 1
NHERF-1	Na^+/H^+-exchanger regulatory factor 1
NSF	N-ethylmaleimide-Sensitive Factor
ON	Over Night
PDZ	Postsynaptic Density/Discs large/Zonula occludens
PFA	Paraformaldehyde

PLA	Proximity Ligase Assay
P/S	Penicillin Streptomycin
RACK1	Receptor for Activated protein C Kinase 1
RE	Recycling Endosome
RT	Room Temperature
SE	Sorting Endosomes
SDS-PAGE	Sodium Dodecyl Sulfate-PolyAcrylamid Gel Electrophoresis
SNARE	Soluble NSF Attachment protein Receptor
SNX27	Sorting Nexin 27
TBST	Tris-Buffered Saline Tween 20
TGS	Tris Glycine SDS
rTetR	tet Repressor
TGN	Trans-Golgi Network
tTA	tetracyclin-controlled TransActivator
VP16	Viron Protein 16
VPS35	Vacuolar Protein Sorting 35
WB	Western Blotting

Table of content

1 Introduction

Normal function of all epithelia relies on the correct polarized localization of ion transport proteins, and malfunctions in the trafficking of these proteins to the plasma membrane contribute to numerous diseases (Mellman and Nelson 2008). Solute carriers (SLCs) were recently called "the most understudied group of genes", because of the discrepancy between the limited number of studies investigating them and their high relevance to health and disease (César-Razquin et al. 2015). One family amongst the SLCs is the *SLC4* family, a large group of distinct and functionally diverse regulators of intracellular pH (pH_i). Regulation of pH_i is essential for the normal function of all organisms since the structure and function of virtually all proteins depends on pH and altered pH functions as signaling in many biological processes (Flinck, Kramer, and Pedersen 2018). Specifically, the widely expressed Na^+, HCO_3^- cotransporter NBCn1 (SLC4A7) is a major regulator of pH_i in most cell types with important functions in the cardiovascular system, the kidneys, and other organ systems (Aalkjaer et al. 2014). Most recently, NBCn1 has been shown to play an essential role in macrophage phagosome acidification (Sedlyarov et al. 2018). The dysfunction of NBCn1 is implicated in hypertension (Ehret et al. 2011) and cancer (Boedtkjer, Bunch, and Pedersen 2012). In particular, NBCn1 plays a central role in breast cancer (Boedtkjer et al. 2013, Lauritzen et al. 2010, Andersen et al. 2016, Gorbatenko et al. 2014, Lee et al. 2015), and genome-wide association studies link a SNP in the NBCn1 3' untranslated region to increased breast cancer risk (Chen, Zhong, et al. 2012). Despite the importance of NBCn1 in physiology and disease, very little is known about the regulation and roles of NBCn1. Specifically, there is a near-complete lack of knowledge regarding NBCn1 biosynthesis, trafficking, and degradation pathways. The aim of this project is, therefore, to investigate NBCn1 sorting and trafficking pathway(s) in epithelial cells and potential interaction partners involved in the membrane expression of NBCn1.

1.1 The Na^+, HCO_3^--cotransporter NBCn1 (SLC4A7)

1.1.1 Molecular actions of NBCn1

The electroneutral Na^+/ HCO_3^--cotransporter, NBCn1, mediates the cellular import of Na^+ and HCO_3^- with a 1:1 stoichiometry (Parker and Boron 2013). When HCO_3^- reacts with intracellular H^+ ions, they form carbonic acid (H_2CO_3), which becomes freely diffusible CO_2 and H_2O in the presents of cytosolic carbon anhydrases catalyze. As CO_2 diffuses out of the cell, membrane-bound carbonic anhydrases catalyze the

hydration of CO_2 to form H_2CO_3, dissociating into HCO_3^- and H^+ outside the cell (Aalkjaer et al. 2014). Essentially, the movement of HCO_3^- becomes functionally equivalent to the movement of H^+ in the opposite direction. Moreover, this allows for the recycling of HCO_3^-, making NBCn1 a net acid extruder.

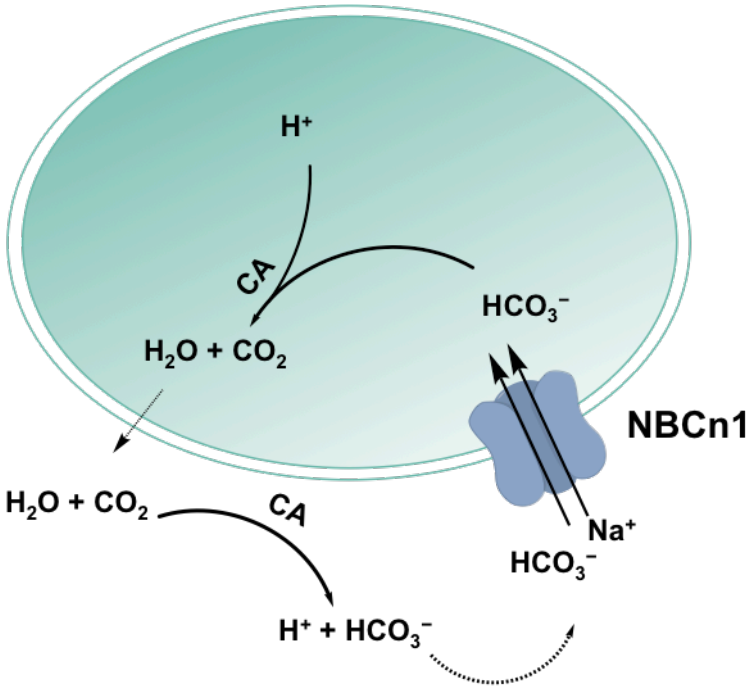

Figure 1 The primary molecular action of the electroneutral Na^+, HCO_3^- cotransporter NBCn1. It fascilitates the import of sodium ions (Na^+) and bicarbonate (HCO_3^-) in the 1:1 stoichiometry. The intracellular H^+ reacts with the imported HCO_3^-, forming H_2O and CO_2. As CO_2 diffuses out of the cell, it is hydrated, a process catalyzed by carbonic anhydrases (CA), resulting H^+ and HCO_3^-. NBCn1 is a net acid extruder because HCO_3^- is recycled into the cell.

In addition to the Na^+/HCO_3^--cotransport, NBCn1 has a unique Na^+-channel-like activity that is independent of HCO_3^-. This was demonstrated in *Xenopus* oocytes expressing the NBCn1-B variant (see section 1.1.3), which were notably depolarized after resting and loaded with more than six times the intracellular Na^+ than the control oocytes (Choi et al. 2000). Supporting this, Choi and colleagues found that NBCn1-expressing oocytes hyperpolarize after removal of the extracellular Na^+ in the nominal absence of CO_2/ HCO_3^- (Choi et al. 2000). However, the primary function of NBCn1 is regulation of pH.

1.1.2 Physiology

NBCn1 knockout mice develop blindness and auditory deficiency due to the missing NBCn1-mediated acid extrution in sensory neurons (Bok et al. 2003). Furthermore, NBCn1 knockout mice have inhibited vasodilation due to reduced NO production in the endothelial cells, making them susceptible to hypertension.

Most likely, this is due to altered intracellular pH affecting the endothelial NO-synthase (Boedtkjer et al. 2011). NBCn1 is widely expressed and thus a major regulator of pH_i in most cell types. One organ system where NBCn1 is notably abundant is the renal system. More specifically, NBCn1 is highly expressed basolaterally in the medullary thick ascending limbs and the inner medullary collecting ducts of the kidneys (Odgaard et al. 2004). Generally, NBCn1 is localized in the basolateral membrane domain of polarized epithelial cells (Olesen et al. 2018, Damkier, Nielsen, and Praetorius 2006), but apical localization has also been reported in choroid plexus epithelium (Praetorius and Nielsen 2006). In the kidneys, it is hypothesized that basolateral NBCn1 counteracts intracellular acid load from $NH4^+$-reabsorption, thereby promoting $NH4^+$-excretion (Odgaard et al. 2004, Praetorius et al. 2004). Another organ system, where basolateral NBCn1 plays an important role, is in the duodenal mucosa of the upper gastrointestinal tract. Here, basolateral NBCn1 activity is proposed to protect the epithelium against the high gastric acid concentrations by raising the intracellular HCO_3^-, and thereby promoting the apical secretion of HCO_3^- by other transporters (Chen, Praetorius, et al. 2012).

1.1.3 Association with Cancer Development

In addition to the important physiological roles, NBCn1 is demonstrated to play a central role in breast cancer (Lee et al. 2015, Boedtkjer et al. 2013). Characteristic for all malignant tumors is uncontrolled proliferation, which leads to a high metabolic rate and hypoxia (Hanahan and Weinberg 2011). Hypoxia alters cell biology for instance via HIF1α, which contributes to a metabolic shift towards aerobic glycolysis, known as the Warburg effect (Swietach et al. 2014). Despite the intracellular acid load from a high metabolic rate, cancer cells tend to have a highly acidic tumor microenvironment and a more alkaline pH_i compared to normal cells (White, Grillo-Hill, and Barber 2017). This reversed pH gradient favors tumor progression because high pH_i stimulates cell proliferation and survival, while low extracellular pH (pH_e) is important for migration and invasion (Flinck, Kramer, and Pedersen 2018). NBCn1 plays an important role in maintaining the altered pH homeostasis in breast carcinomas (Lee et al. 2015). In fact, CO_2/ HCO_3^--dependent mechanisms were shown to beresponsible for more than 90% of the total acid extrusion in freshly dissected human patient breast cancer tissue when pH_i is higher than 6.6 (Boedtkjer et al. 2013). In congruence with this, NBCn1 expression and function are increased in breast cancer tissue compared to normal breast tissue (Boedtkjer et al. 2013, Lee et al. 2015). The importance of NBCn1 in breast cancer is further validated by the reduced steady state pH_i in NBCn1 knock-down (KD) cells and *in vivo* evidence of NBCn1 KD reduced tumor growth of triple-negative breast cancer cell xenografts in mice and prolonged tumor-free survival (Andersen et al. 2018).

1.1.4 Structure of NBCn1

Despite the central role of NBCn1 in physiology and disease, very little is known about the molecular mechanisms behind its localization and function. There is no structure of NBCn1 available, but the topology is predicted from the AE1, the first structure in the SLC4 family (Arakawa et al. 2015), to consist of a large cytosolic N-terminus of approximately 400 kDa, a transmembrane domain (TMD) with 14 α-helical spans plus an extended glycosylated extracellular loop between transmembrane span 5 and 6, and a smaller cytosolic c-terminus of aproximately 100 kDa (Parker and Boron 2013). The most distal part of the C-terminus contains a PDZ-binding domain (ETSL), which is important for the interaction with other cellular components (elaborated in section 1.1.6). The cytosolic C-terminal domain is vital for the stable NBCn1 membrane localization, and several groups, including ours, have shown that deletion of the C-terminus, but not the PDZ binding motif alone, abolishes the membrane localization possibly due to intracellular retention (Loiselle, Jaschke, and Casey 2003, Olesen et al. 2018, Arakawa et al. 2015). However, nothing is known about the mechanisms involved.

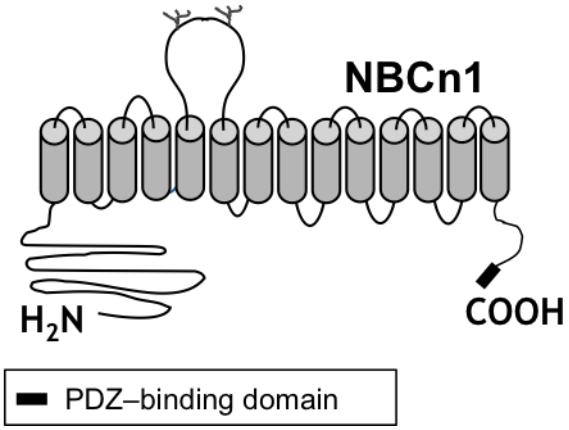

Figure 2 The predicted structure of NBCn1. A large cytosolic N-terminal domain (400 kDa), a transmembrane domain with 14 α-helical spans with an extended glycosylated extracellular loop between span 5 and 6, and a smaller cytosolic C-terminal domain (100 kDa). The most distal part of the C-termins contains a PDZ-binding domain important for the interaction with other cellular components. Source: Modified from original by Professor Stine F. Pedersen.

1.1.5 NBCn1 Splice Variants

Due to alternative promoter sites, two distinct NBCn1 N-termini exist. One containing Exon 1 (16 amino acids) beginning with the sequence MEAD, the other containing exon 2 (11 amino acids) beginning with the sequence MERF (**Figure 3**) (Parker and Boron 2013, Gorbatenko et al. 2014). The physiological consequence of the two promoter sites is not known. It is, however, highly relevant for experimental work as

many antibodies raised against NBCn1 target the cytosolic domains. For instance, important studies of NBCn1 tissue-specific expression levels by Damkier and colleagues have been performed using antibodies targeting the MEAD sequence, which is predicted to leave out expression patterns of NBCn1 containing exon 2 (NBCn1-A,F,J-L) (Boedtkjer, Bunch, and Pedersen 2012). In addition to the alternative promoter sites, cytosolic splicing events result in at least three different splicing cassettes (cassette I-III) (**Figure 3**). Cassette I and II are located in the N-terminal domain, whereas cassette III is located in the C-terminal domain. Casette I contains 13 amino acids and variants with and without cassette I appear to be coexpressed in most tissues (Damkier, Nielsen, and Praetorius 2006). Cassette II consists of 124 amino acids and is predominately expressed in vascular smooth, cardiac, and skeletal muscle cells, but absent from most epithelia (Damkier, Nielsen, and Praetorius 2006). In most tissues, variants expressing cassette III are dominant, but low levels of variants lacking cassette III are also frequently detected (Damkier, Nielsen, and Praetorius 2006). The functional importance of the different NBCn1 variants is largely unknown, although further studies might provide knowledge of tissue-specific regulation of the NBCn1 (Boedtkjer, Bunch, and Pedersen 2012).

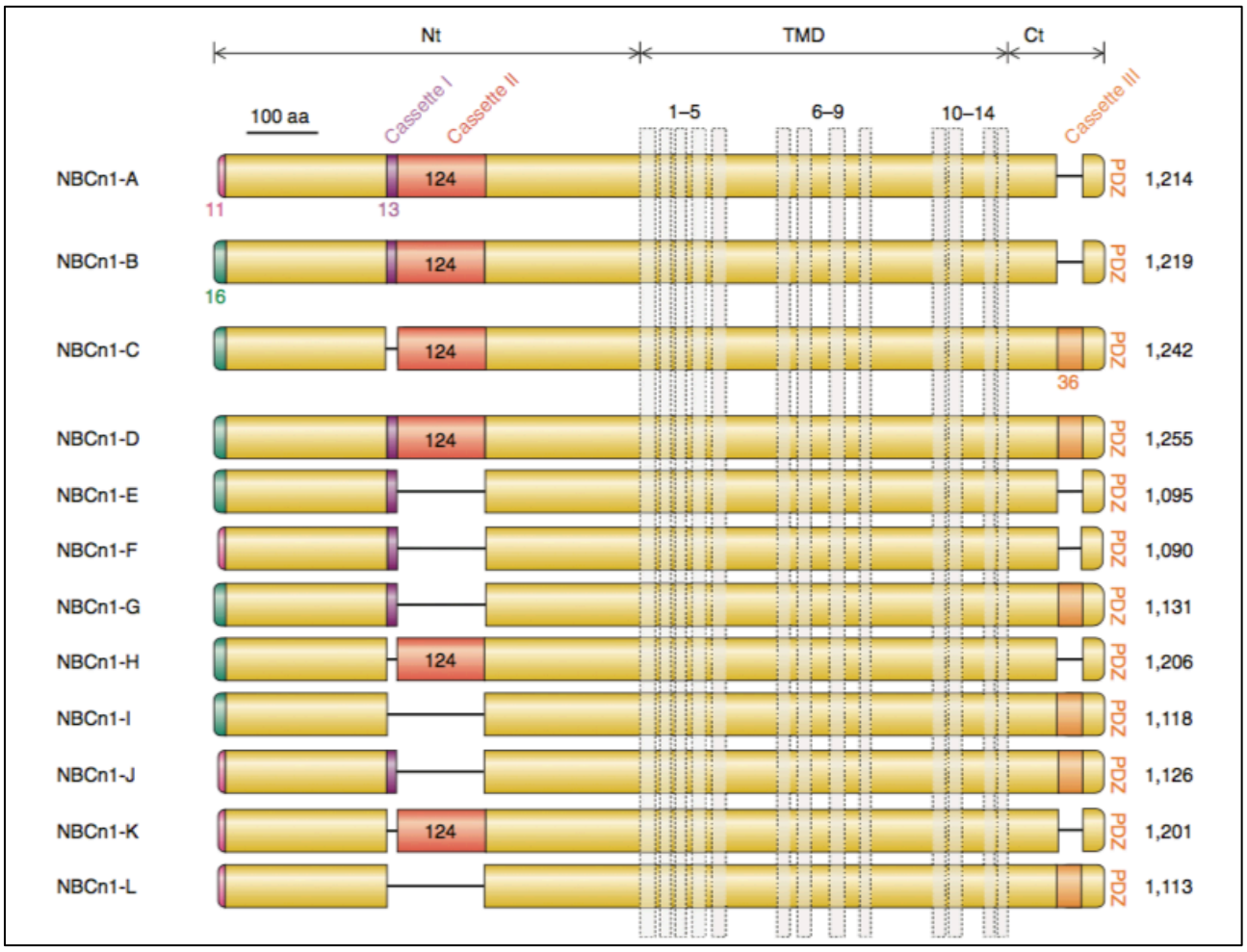

Figure 3 NBCn1 splice variants (NBCn1-A-L). Alternative promoter sites are responsible for the two distict starting sequences of the NBCn1 N-terminus: MERF (11 amino acids, pink) and MEAD (16 amino acids, green). Cassette I (purple) is 13-amino acids long, cassette II (red) contains 124 amino acids. They are both located in the N-terminus, whereas the 36-amino acid long cassette III (orange) is located in the C-terminus. Furthermore, the most distal part of the C-terminal domain contains a PDZ-binding domain important for NBCn1 interaction with other cellular components. Nt: N-terminal, TMD: Transmembrane domain, Ct: C-terminal. Source: (Parker and Boron 2013).

1.1.6 Interaction with other cellular components

The PDZ-binding domain of the NBCn1 c-terminus interacts with scaffold protein Na^+/H^+-exchanger regulatory factor 1 (NHERF-1), linking NBCn1 to other transport proteins (Saras and Heldin 1996). In the N-terminus, the cassette II domain of NBCn1 interacts with Ca^{2+}-dependent phosphatase calcineurin, possibly a mechanism for tissue-specific regulation (Danielsen et al. 2013). Furthermore, the NBCn1 N-terminus interacts with IP_3 receptor binding protein released with inositol 1,4,5- triphosphate (IRBIT), a signaling molecule, which has been shown to increase the rate of NBCn1-mediated pH_i recovery in *Xenopus* oocytes (Boedtkjer, Bunch, and Pedersen 2012).

1.2 Sorting and trafficking of NBCn1 in polarized epithelial cells

Prior to this study, our lab performed mass spectrometry analysis of interaction partners of both the N- and C-termini of NBCn1, to begin to resolve the mechanisms of NBCn1 regulation. Here, I focus on the C-terminal partners. Several putative NBCn1 interaction partners with roles in protein trafficking, sorting, and turnover were revealed by GST pulldown with the NBCn1 C-tail (Olesen et al. 2018). As this project serves to validate some of these interaction partners, this section focuses on the functions of these proteins in basolateral sorting.

1.2.1 General sorting of newly synthesized membrane proteins to the basolateral membrane

Newly synthesized proteins are transported between the intracellular organelles in vesicles formed from specialized, coated regions in membranes of each compartment. First, nascent proteins are transported from the endoplasmic reticulum (ER) to the Golgi apparatus in coatamer complex-II (COPII)-coated vesicles. From the trans-Golgi network, epithelial membrane proteins are recognized by adaptor protein (AP) complexes and transported in clathrin-coated vesicles to the plasma membrane directly or, alternatively, through recycling endosomes (REs) before reaching the plasma membrane (Farr et al. 2009, Ang et al. 2004).

1.2.2 Adaptors and sorting motifs for basolateral proteins

APs are key regulators of vesicular transport as they recognize intrinsic protein sorting signals and concentrate cargo proteins into patches. This is dependent on their ability to recruit and bind clathrin. Clathrin gathered by Aps, self-assembles into cage-like structures, forming coated buds from the membrane, resulting in transport vescile formation (Duffield, Caplan, and Muth 2008). There are five different AP complexes (AP1-5) with specific sorting function at distinct intracellular organelles. Each AP complex consists of two large subunits (one α, γ, δ, ε, or ζ and one β1-5), one medium (μ1-5), and one small (σ1-5) (Park and Guo 2014). The epithelial-specific variant of the AP-1 complex, AP-1B (γ, β1, μ1B, σ1), is involved in basolateral targeting (Fölsch et al. 1999, Gan, McGraw, and Rodriguez-Boulan 2002), yet not all epithelial cells express AP-1B and AP-4 (ε, β4, μ4, σ4) may also play a role (Simmen et al. 2002, Fölsch 2005). AP-1B is localized at the TGN and REs in polarized cells and the selective localization to specific intracellular organelles is controlled by the interaction between APs and phosphoinositides on the membranes (Park and Guo 2014).

AP-1 recognizes tyrosine-based sorting motifs (YXXØ), dileucine-based hydrophobic signals ([DE]XXXL[LI]) (X is any amino acid and Ø is hydrophobic amino acid), and non-canonical basolateral sorting motifs (including acidic clusters) (Park and Guo 2014, Mellman and Nelson 2008). The NBCn1 cytosolic C-tail contains no such canonical motifs. However, it does contain an acidic cluster and two regions resembling leucine-based sorting motifs **Figure 4**.

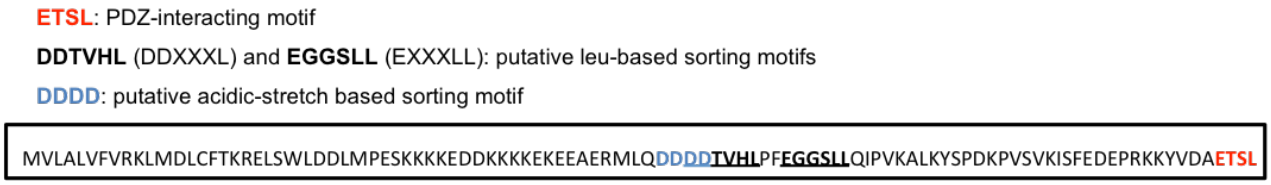

Figure 4 Putative non-canonical sorting motifs in the NBCn1 C-tail.

1.2.3 Tethering and fusion with the basolateral membrane

Another protein complex with potential relevance for the sorting of NBCn1 to the basolateral membrane is the exocyst complex (Sec3, Sec5, Sec6, Sec8, Sec10, Sec15, Exo70, and Exo84). Exocyst is involved in the docking and tethering of some transport vesicles from the TGN to the basolateral membrane and is, moreover, associated with AP-1B clathrin-coated vesicles (Grindstaff et al. 1998). The exact function of exocyst is not clear, but the Sec6 and Sec8 components are recruited restrictedly to the lateral membrane in MDCK-II cells (Grindstaff et al. 1998), where it might mediate tethering of transport vesicles through interaction with $PI(4,5)P_2$ (Wu and Guo 2015). The association of exocyst with AP-1B clathrin-coated

vesicles, and thus basolateral sorting, is regulated by the small GTPases Cdc42, RalA, Rab8, and Rab10 (ref?). These GTPases interact with exocyst (Kang and Fölsch 2009, Moskalenko et al. 2002), microtubules, and motor proteins moving the vesicles (Fölsch 2005).

Final fusion of transport vesicles with the plasma membrane is mediated by interaction between a set of v-SNARE proteins on the vesicle and three sets of complementary t-SNAREs on the target membrane (Wu and Guo 2015, Jahn and Scheller 2006). These SNAREs contribute to an extra layer of vesicle fusion specificity. For basolateral sorting, the t-SNARE syntaxin-4 is important (Mellman and Nelson 2008).

Based on this and the LC-MS/MS data, we speculate that NBCn1 is translocated to the basolateral membrane either directly from the TGN or via recycling endosomes, possibly in AP-1B (γ, β1, μ1B, σ1) clathrin-coated vesicles, which might involve Ral-A, Rab8a, Rab10, exocyst, and syntaxin-4 (**Figure 5**). However, before the start of my project, none of these putative interactions had yet been validated.

1.2.4 Lateral membrane targeting and retention in polarized epithelial cells

Although NBCn1 is basolateral in most epithelial cells (Olesen et al. 2018, Loiselle, Jaschke, and Casey 2003), NBCn1 is strikingly lateral in MDCK-II cells grown on Transwell filters compared to another basolateral solute carrier, the Na^+/H^+ exchanger NHE1 (SLC9A1) (Olesen et al. 2018), suggesting a different targeting pattern. The ability of epithelial cells to maintain two different membranes with distinct composition of ion transport proteins is essential for the barrier function of all epithelia. The apical and the basolateral membrane are separated by intercellular tight junctions (Mellman and Nelson 2008). Tight junctions contain the transmembrane proteins occludin and claudins and maintain polarity, together with adherence junctions below them, by binding directly to protein partners in the neighbouring cells and preventing membrane proteins from diffusing from one membrane to the other (Nejsum and Nelson 2009). In addition to these intercellular junctions, three other protein complexes are required for cell polarity establishment: partitioning defective (PAR), Crumbs, and Scribble (Mellman and Nelson 2008, Iden and Collard 2008). They provide orientational cues and regulate the identity of the apical and basolateral membranes by antagonizing each other. The Scribble complex, comprising Scribble, lethal giant larvae (LGL), and discs large (DLG), is localized below the adherence junctions along the lateral membrane, from where it regulates the basolateral membrane identity (Tanentzapf and Tepass 2003, Iden and Collard 2008, Bilder, Schober, and Perrimon 2003). The Scribble complex is also thought to be important for basolateral sorting, probably due to interactions between LGL and syntaxin-4 (Müsch et al. 2002) and, as found in yeast, additional interaction between LGL and exocyst (Bilder, Schober, and Perrimon 2003).

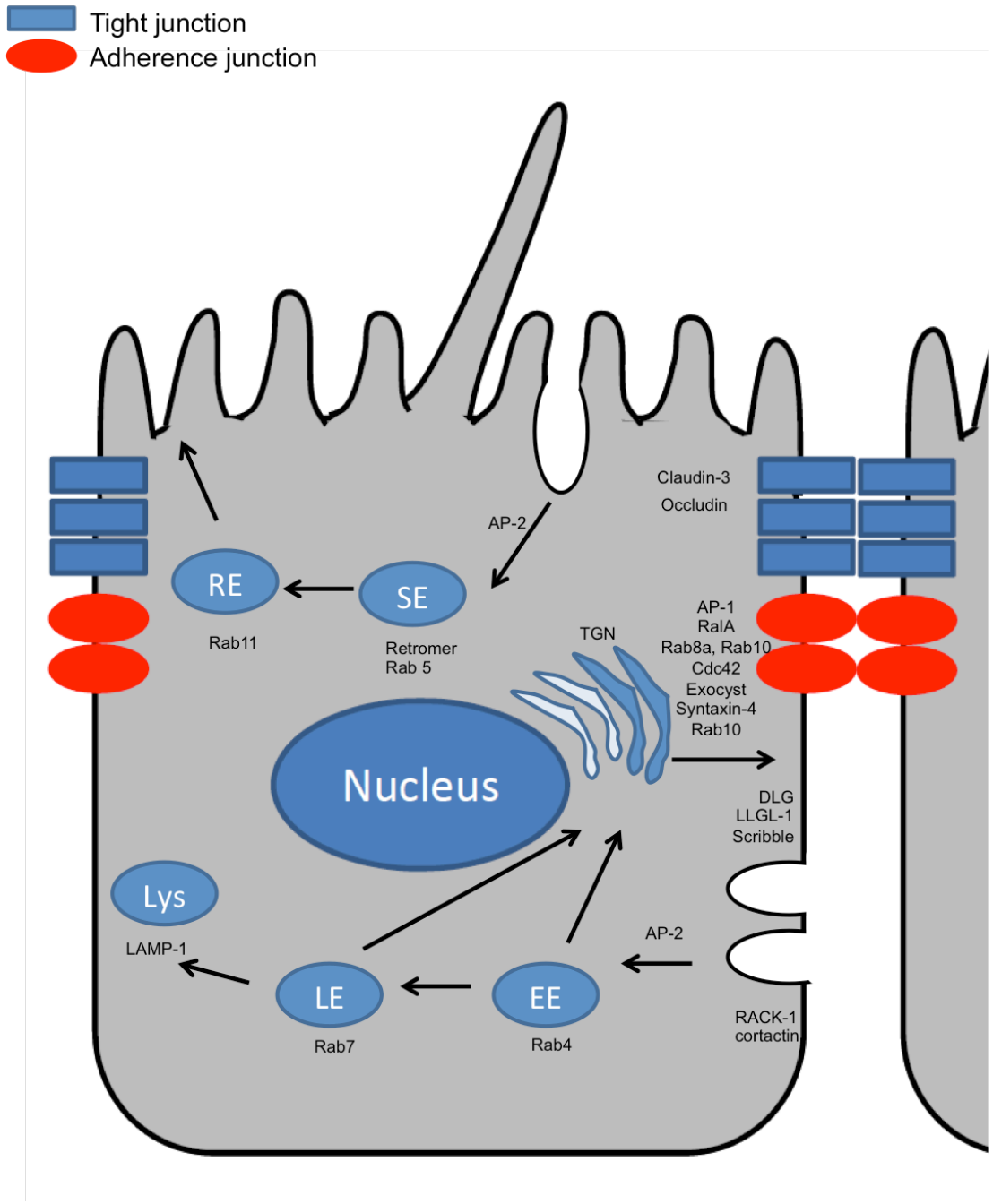

Figure 5 Trafficking in polarized epithelial cells. RE: Recycling endosomes, SE: Sorting endosomes, EE: Early endosomes, LE: Late endosomes, LYS: Lysosome, TGN: Trans-Golgi Network. Modified from Stine F. Pedersen

Another interesting putative NBCn1 interactor revealed by the MS analysis, is the cytoplasmic scaffolding protein receptor for activated C-kinase-1 (RACK1), which is implicated in the trafficking and retention of several other ion transporters (Ohgaki et al. 2008, Onishi et al. 2007, Parent et al. 2008). RACK1 is particularly interesting as our lab validated interaction with NBCn1 by proximity ligation assay (PLA) in

T47D cells (Olesen et al. 2018). Lastly, the scaffold for F-actin regulation cortactin was identified from the LC-MS/MS data. Cortactin is also involved in the membrane localization of other transport proteins (Herrmann et al. 2012).

Collectively, this indicates potential roles for occludin, claudins, Scribble, LGL, DLG, RACK1, and cortactin in the targeting and retention of NBCn1 in polarized epithelial cells (**Figure 5**).

1.2.5 Retrieval, sorting, and turnover of proteins from the basolateral membrane

The regulation of plasma membrane expression levels involves internalization via endocytosis. Endocytosis can be clathrin-dependent or -independent. The process of clathrin-dependent endocytosis is divided into 5 steps: nucleation, cargo selection, coat assembly, scission, and uncoating (McMahon and Boucrot 2011, Traub 2009). A nucleation module is assembled when proteins, such as FCH domain only (FCHO) and EGFR pathway substrate 15 (EPS15), bind to $PI(4,5)P_2$ together with AP-2 (α, β2, μ2, σ2), which is responsible for the cargo selection, allowing clathrin coat assembly by cargo adaptor and curvature effector AP180. In clathrin-dependent endocytosis dynamin is responsible for the scission, but dynamin-dependent, clathrin-independent endocytosis also occurs, typically via caveolae (Mayor and Pagano 2007). The last endocytosis pathway is dynamin- and clathrin-independent, and relies on the microtubule motor dynein and the dynactin complex, which is necessary for dynein function (Day et al. 2015). All endocytosed vesicles eventually meet at the early endosomes, containing Rab5 (Duffield, Caplan, and Muth 2008, Mayor and Pagano 2007). From here, endocytosed membrane proteins can be recycled back to the plasma membrane though Golgi or to sorting endosomes (SEs), from where they again can be recycled back to the plasma membrane or sorted further on to REs or late endosomes (LEs), ending up in the lysosomes for degradation (Duffield, Caplan, and Muth 2008).

MS analyses have also shown NBCn1 interaction with retromer components VPS35 and SNX27. Retromer localizes to the SE and directs endocytosed membrane proteins (Seaman, Gautreau, and Billadeau 2013). AP-2 components, dynactin, early endosom-associated Rab 4 and Rab5, late endosome-associated Rab7, VPS35 and SNX27 were revealed as putative NBCn1 interaction partners by the MS analysis. Interestingly, Rab11, which is localized on the REs, was also strongly suggested (Olesen et al. 2018) (**Figure 5**).

2 Aim

The overall aim of this project was to increase the understanding of the sorting, targeting and trafficking of the pH-regulatory transporter NBCn1 in normal epithelial cells.

The work had the following specific objectives:

- To investigate the trafficking of newly synthesized NBCn1 to the plasma membrane.
- To validate NBCn1 interaction partners involved in the sorting, targeting and trafficking of NBCn1.
- To gain knowledge of NBCn1 interaction domains. Materials and Methods

3 Materials and methods

3.1 Experimental overview

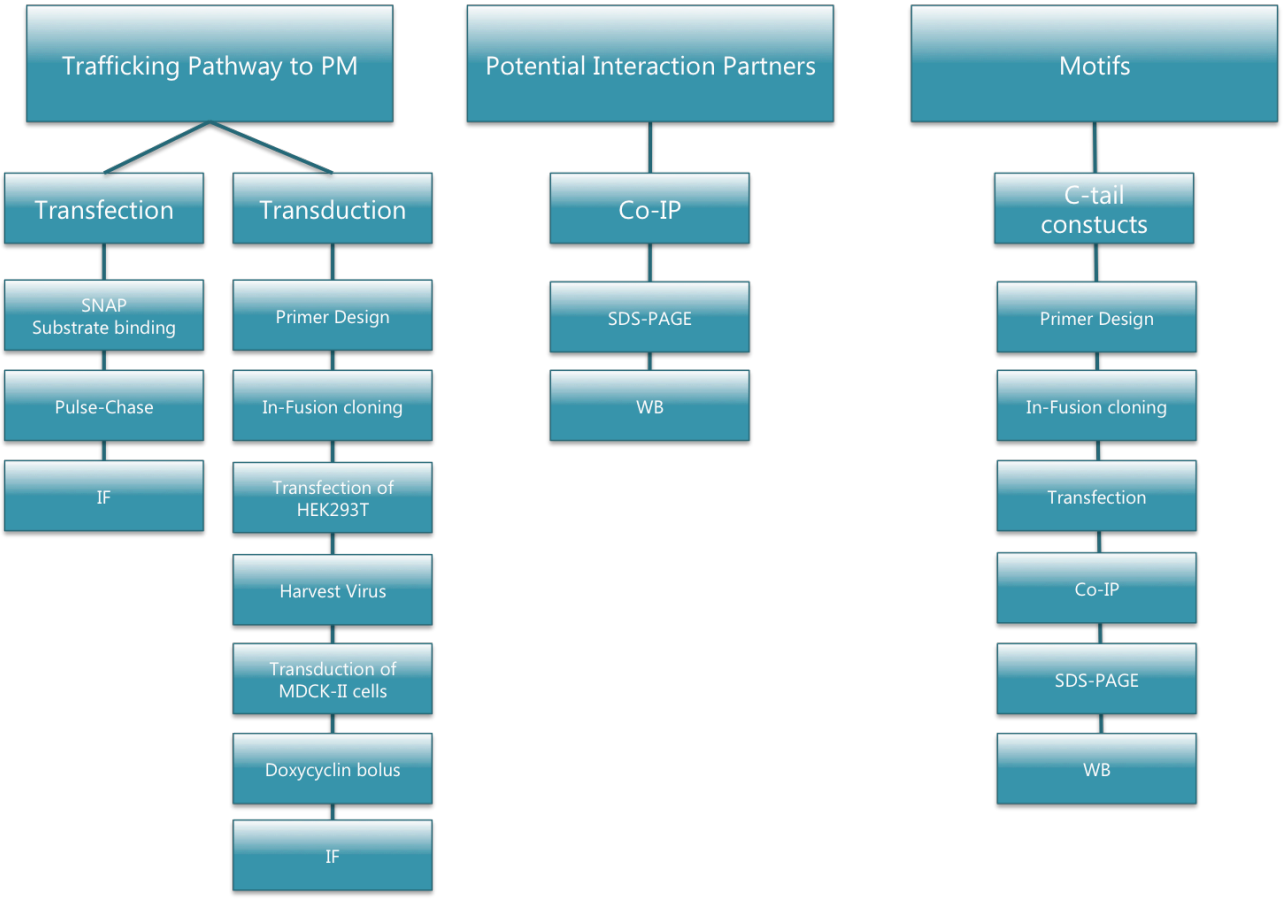

Figure 6 Experimental overview to illustrate the order in which the experiments were carried out.

3.2 Antibodies

The primary antibodies used in this project are listed below. For co-IP, many antibodies were used according to the amount of protein in the samples. ”1 µg /mg” is 1 µg /mg protein in the sample.

Antigen	Species	Cat. no.	Co-IP	WB	IF
AP180	Rabbit pol	Abcam #33898	1 µg /mg		
B-actin	Mouse mon	Sigma-Aldrich #A5441		1:20,000	
Claudin 3	Rabbit pol	Abcam #52231	1.25 µg /mg		
DLG (SAP97)	Rabbit pol	Abcam #3437	1:50 (v/v)		
Cortactin (Y421)	Rabbit pol	Abcam #47768	1 µg /mg		
α-adaptin	Mouse mon	Abcam #2730	1 µg/mg		
FLAG M2	Mouse mon	Sigma-Aldrich #F1804			
γ-adaptin	Rabbit	Abcam #21980	1:100 (v/v)		
HA-Probe	Rabbit pol	SantaCruz, discontinued			1:200
LAMP-1 (H4A3)	Mouse mon	Santa Cruz #20011	1 µg/mg		
LLGL-1	Rabbit mon	Abcam #183021	3.78 µg /mg		
NBCn1 (nt)	Rabbit	Gift from J. Prætorius	2 µL/mg	1:1,000	1:200
NBCn1 (ct)	Rabbit pol	Abcam #82335	1 µg/mg		
IgG	Rabbit	Cell Signaling #2729	1 µg/mg		
IgM	Mouse	eBioscience #14475282	1 µg/mg		
Rab4	Rabbit pol	Abcam #13252	1 µg/mg		
Rab7	Rabbit mon	Cell Signaling #9367	1:100 (v/v)		
Rab10	Rabbit mon	Cell Signaling #8127S	1:50 (v/v)		
Rab11	Rabbit mon	Cell Signaling #5589S	1:50 (v/v)		
RACK1	Mouse	BD Biosciences #610177	1.25 µg/mg	1:1,000	
SNX27	Mouse mon	Abcam #77799	1 µg/mg		
Scribble	Rabbit pol	Cell Signaling #4475S	1:50 (v/v)		
VPS35	Rabbit pol	Abcam #97545	1 µg/mg		

3.3 Cell lines

3.3.1 MDCK-II cells

In the present study, the Madin-Darby Canine Kidney II (MDCK-II) cell line was employed as a model to study the trafficking of NBCn1 to the plasma membrane. MDCK-II cells are isolated from normal kidney tubule and is therefore not considered a cancer cell line. In paticullar, this cell line is great for the study of mechanisms in polarized epithelial cells as they exhibit the ability to polarize and resemble renal tubles in a dish (Hall, Farson, and Bissell 1982). MDCK-II cells were cultured in Minimum Essential Medium Eagle (MEM) Alpha Modifications (Sigma, #M8042) with 10% heat-inactivated fetal bovine serum (FBS; Gibco, #10 106-177), 1% penicillin/streptomycin (P/S; Invitrogen, # 15140-148), and 2 mM L-Glutamine (Gibco #25030081).

3.3.2 HEK293 and HEK293T cells

HEK293 are transformed human embryonic kidney cells from normal tissue (Graham et al. 1977). HEK293 cells were employed for pulse-chase experiments as a positive control for transfection as the transfection efficacy is generally greater in HEK293 cells compared to MDCK-II cells. However, this cell line is only semi-adherent and tend release from the surface on which they are grown when fully confluent or grown on coverslips. HEK293T cells were employed for lentiviral production. The HEK293 cell line is derived from the HEK293 cell line, but express the temperature sensitive SV40 large T antigen. Plasmids containing the SV40 origin of replication can maintain a high copy number, which increases the amount of virus produced in these cells (ATCC). Both cells line were cultured in Dulbecco's Modified Eagle Medium (DMEM 1X) with 4.5 g/L D-Glucose, L-Glutamine, and Pyruvate (Gibco, #41966-029) with 10% heat-inactivated fetal bovine serum (FBS; Gibco, #10 106-177) and 1% penicillin/streptomycin (P/S; Invitrogen, #15140-148).

Maintenance of cell cultures

Cells were grown in T75 flasks (Cellstar, #658 170) or T175 (Cellstar, 660 175) at 37°C, 5% CO_2, and with 95% humidity. To maintain continuos cell proliferation, cells were passaged in a ratio of 1:20 (v/v) for MDCK-II cells and 1:10 (v/v) for HEK293 cells upon reaching 80-100% confluency. Passage was performed according to the following procedure: Growth medium was removed. To remove remaining growth medium containing trypsin protease-inhibiting proteases from the FBS and trypsin-inhibiting Mg^{2+} and Ca^{2+}ions, cells were washed twice in PBS (Appendix I - Solutions). Cells were then exposed to Trypsin-EDTA (Appendix I - Solutions) for 5-10 min depending on the cell line, MDCK-II cells being exposed the longest. Cells were then resuspended in media, inactivating the trypsin. After approximately 30 passages,

cells were discarded.

3.4 Immunofluorescence

Cells were washed in ice-cold PBS (and fixed for 30 min. in 4% PFA on ice. After fixation, cells were washed twice for 5 min in TBST (Appendix I - Solutions). Fixed cells were permeabilized for 5 min in 0.5% triton-X-100 (Plusone, #17-1315-01) diltued in TBST and blocked for 30 min in 5% bovine serum albumin (BSA; Sigma-Aldrich, #A7906-50G) diluted in TBST. Next, cells were incubated for 1.5 h in primary antibody diluted in TBST containing 1% BSA at RT in humid chamber. Cells were washed three times for 5 min in TBST containing 1% BSA and incubated for 2 h in appropriate Alexa Fluor secondary antibody, and in some cases rodhamine phalloidin (Invitrogen) 1:100, diluted 1:600 in washing solution at RT in humid chamber. Cells were washed once in washing solution, nuclei were stained for 5 min with µM DAPI (Invitrogen), followed by additional three washes and mounting in 2% (w/v) N-propyl-gallate (Sigma-Aldrich, #P-3130) diluted in UltraPure glycerol (Invitrogen, #15514-011) with 10% PBS. Images were obtained on a 60x oil objective using Cell Sense software and were processed in ImageJ.

3.5 Post-fixation SNAP-tag labeling with BG-549

For post-fixation SNAP-tag labeling, MDCK-II cells seeded to be 50-60% confluent when transiently transfected with the NBCn1-SNAP-HA using Lipofectamine 2000 (Invitrogen, #11668-019) in a ratio of 1:5 (w/v) DNA to Lipofectamine. After 24 hrs, cells were washed with 1mM $MgCl_2$ and 100 µM $CaCl_2$ (PBS^{2+}) followed by fixation for 30 min in 4% paraformaldehyde (PFA, Sigma-Aldrich, #47608) on ice. After fixation, cells were washed again in PBS^{2+}. Fixed cells were permeabilized and blocked in PBS^{2+} containing 10% FBS, 0.5% BSA, and 0.2% saponin (Sigma-Aldrich, #47036) for 30 min at RT. Next, cells were incubated for 1 h in ntNBCn1 antibody or HA-Probe (0) and 5 µM cell impermable substrate BG-549 (NEB, #S9112S) diluted in blocking solution. Cells were washed three times for 10 min in PBS2+ containing 1% BSA and 0.2% saponin and incubated for 1 h in appropriate Alexa Fluor secondary antibody diluted in blocking solution, followed by additional two washes. For nuclei staining, cells were incubated for 5 min in DAPI (Invitrogen) diluted in washing solution, washed two times for 5 min in washing solution, rinsed two times for 5 min in PBS2+, and mounted in 2% (w/v) N-propyl-gallate (Sigma-Aldrich, #P-3130) diluted in UltraPure glycerol (Invitrogen, #15514-011) with 10% PBS. Images were obtained on a 60x oil objective using Cell Sense software and processed in ImageJ.

3.6 Live SNAP-tag labeling with TMR-Star SNAP-Cell

For live SNAP-tag labeling, MDCK-II cells seeded to be 50-60% confluent when transiently transfected with Lipofectamine 3000 (Invitrogen, #L3000-015) the NBCn1-SNAP-HA using in a ratio of 1:5 (w/v) DNA to Lipofectamine. After 24 hrs, cells were labled for 30 min with 3 µM cell-permable TMR-Star fluorescent SNAP-Cell substrate (NEB, S9105S) dissolved in complete medium at 37℃ and 5% CO_2. Cells were washed additional three times in complete medium followed by incubation for 30 min in complete medium. Medium was replaced once more to remove the unreacted substrate that had difussed out of the cells and immunofluorescence was carried out as described in section 0. For the SNAP-block experiments, the SNAP-tag reactivity was blocked for 20 min in 10 µM SNAP-Cell Block (NEB, #S9106) dissolved in complete medium (see section 3.3.1). Cells were washed three times in complete medium and then labled.

3.7 Lentiviral transduction

3.7.1 Primer design

Primer for site-directed cloning of respectively NBCn1-SNAP-HA (IAX-FWD-1 and IAX-REV-2) and GFP-NBCn1 (IAX-FWD-5 and IAX-REV-6) into lentiviral backbone plasmid pCW57.1 (Addgene, #41393) were designed according to the In-Fusion HD Cloning Kit guidelines (Takara Bio, #121416) (**Table 1**). That is, the 5' end of every primer was designed to contain 15 bases homologeus to the vector to which the gene of interest was joined. Additionally, the 3' end of every primer was intended to be gene-specific, between 18-25 bases in length, have GC-content between 40-60%, have a melting temperature (T_m) between 58-65℃, contain no identical runs of nucleotides, and carry maximum two guanines or cytosines within the last five nucleotides. The 3' end properties are shown in Appendix III - Primers and deviations from the guidelines are marked in red. Gene-specificity was ensured using primer-BLAST (www.ncbi.nlm.nih.gov/Blast/). numbered between 1-6 were synthesized by Tag Copenhagen and primers numbered between 10-16 were synthesized by Eurofins.

Primer name	Primer sequence
IAX-FWD-1	5' CGCCTGGAGAATTGGGCCACCatggaggcagacggggcc 3'
IAX-REV-2	5' GTGGTGGTGGACCGGagcgtaatctggaacatcgtatggg 3'
IAX-FWD-5	5' CGCCTGGAGAATTGGatggtgagcaagggcgag 3'
IAX-REV-6	5' GTGGTGGTGGACCGGttacaatgaagtttcagcatccatg 3'

IAX-FWD-10	5' TTGCGGCCGCGAATTccatgatggttcttgcattagtc 3'
IAX-REV-12	5' TCTAGAGTCGACTGGtttcttactttctggcatgagg 3'
IAX-REV-13	5' TCTAGAGTCGACTGGcttctccttcttcttcttgtcatc 3'
IAX-REV-14	5' TCTAGAGTCGACTGGctgggcagttttggccattt 3'
IAX-REV-15	5' TCTAGAGTCGACTGGtgtgagtgtgacaataaatttcgaa 3'
IAX-REV-16	5' TCTAGAGTCGACTGGcaatgaagtttcagcatccatg 3'

Table 1 Primers used for PCR-generated inserts. Higher cases represent the 15-bp sequence overlap complementary to the vector, whereas lower cases represent the sequence complementary to the insert. IAX-FWD1 contains a kozac sequence marked in teal.

3.7.2 In-Fusion cloning

For vector linearization, 1 µg pCW57.1 was incubated for 1 h in NEBuffer 1.1 (NEB, #B7201S) containing 10 units of each of the restriction enzymes AgeI (#R0552S) and NheI (#R0131S). The reaction was carried out in 50 µL, diluted in nuclease-free water. After digestion, the linearized vector was purified from a 1% agarose gel with 1:1000 GelRed (Biotium) by gel purification (Macherey-Nagel, #740609).

PCR mix	
Reagent	**Final Concentration**
CloneAmp HiFi PCR Premix	X 1
Fwd Primer (10 µM)	0,3 µM
Rev Primer (10 µM)	0,3 µM
Template DNA (1000-fold dilution)	1 ng
Sterilized destilized water	
Total:	25 µL

Table 2 PCR mix for insert amplification

The two inserts were amplified according to the CloneAmp HiFi PCR Premix Protocol (Takara Bio, #092612) with 1 ng template DNA for plasmid DNA **Table 2**. The PCR cycles were also found in this protocol **Table 3**. Inserts were run on a 1% agarose gel and purified as described for the linearized vector. For In-Fusion cloning, 100 ng of both insert and vector were incubated for with In-Fusion Enzyme HD Premix provided in the In-Fusion HD Cloning Plus kit (Takara, #638910). The reaction was incubated at 50°C for 15 min and placed on ice together with positive and negative control reactions provided in the kit.

PCR		
Cycles	**Time (sec)**	**Temperature (°C)**
35	10	98
	15	55
	22	72

Table 3 PCR cycles for insert amplification for later In-Fusion cloning.

After In-Fusion cloning, the newly formed constructs were transformed into Stellar Competent Cells provided by the In-Fusion HD Cloning Plus kit (Takara, #638910). For this, 2.5 µL In-Fusion reaction was added to the competent cells, following 30 min incubation on ice, heat shock for 45 sec at 42°C, and incubation on ice again for 2 min. The final volume was brought to 500 µL diluted in provided SOC medium, which was then plated on 100 µg/mL ampicillin agar plates. After 24 hrs, several colonies were selected for miniprep accordin to manufacturer's protocol (Omega, #D6945-01). The Contructs were sequenced by Eurofin and transiently transfected into MCF-7 cells to ensure expression.

3.7.3 Lentivirus production

HEK293T cells were transfected with pCW57.1-NBCn1-SNAP-HA or pCW57.1-GFPNBCn1, envelope plasmid pMD2.G, and packaging plasmid pBR8.91 and incubated in the GMO2 lab. After 48 hrs, virus was harvest and filtered using 0.45 µm syringe filters and MDCK-II cells were incubated with virus for 48 hrs for transduction, following media shift.

3.8 Co-immunoprecipitation

Physical interaction between NBCn1 and potential interactors was investigated by co-immunoprecipitation (co-IP). For native co-IP, MDCK-II cells were subjected to co-IP when 70%, 100%, or fully polarized, depending on the interaction of interest. To extract antigens, cells were washed twice in PBS (**Fejl! Henvisningskilden blev ikke fundet.**) and lysed in 1% IGEPAL CA-630 (Sigma, cat. #I8896) with 50 mM Tris pH 7.4, 140 mM NaCl, 3 mM Na_3VO_4, Phosphatase Inhibitor cocktail (PhosStop; Roche, #04906845001), and Protease Inhibitor cocktail (cOmplete; Roche, #11697498001). Lysate was collected in precooled Eppendendorf tubes with a rubber policeman, incubated for 15 min on ice, gently homogenized with a syringe (0,5 mm needle), and centrifuged for 20 min at 20,000 × *g* at 4°C. Protein content of each sample was quantified (see section 3.9.1) and normalized to a concentration of 2 mg/mL diluted in lysis buffer. For input loading samples, 100 µg protein was collected from each normalized sample. Next, samples

were incubated ON with appropriate antibody on roter at 4°C to allow the formation of immune complexes. For capturing immune complexes on a solid phase matrix, immobilized Protein G crosslinked magnetic beads (Dynabeads Protein G; Invitrogen, #10004D) were washed twice for 10 min in lysis buffer (without PhosStop and cOmplete) on roter at 4°C followed by incubation of immune complexes for 45 min in 1.5 mg Dynabeads on roter at 4°C. Using a magnetic rack, unbound protein was collected and transferred to new precooled Eppendorf tubes. Dynabeads with bound pull-down protein were washed five times for 5 min in lysis buffer (w/o PhosStop and cOmplete). To denature pulldown, Dynabeads were resuspended in 2x NuPAGE LDS sample buffer (Invitrogen, #NP0007) containing 250 mM DTT, and boiled for 5 min at 95°C. Bait protein interactors were allowed to elute for 30 min ice after thorough whirly mixing. Pulldown, input, and (for some experiments) unbound protein were separated by SDS-PAGE (see section 3.9) and analyzed by Western blotting (see section 3.9).

3.9 SDS-PAGE and Western blotting

3.9.1 Protein Determination

Protein concentrations of lysates were determined using Bio-Rad DC Protein Assay (Bio-Rad, #500-0113-15). First, a standard curve was made from a dilution series of BSA (Thermo-Fisher, #23209) in lysis buffer. For each sample, 2.5-5 µL lysate was diluted in lysis buffer to a total volume of 25 µL. 125 µL working reagent (1:50 Reagent S and Reagent A from the kit) was added to both the samples and the standards. 1 mL Reagent B provided from the kit, was added while whirly mixing and protected from light. After 15 min incubation at RT, the absorbance at 750 nm was measured on a Beckman Coulter DU800 spectrophotometer. Samples were normalized to a protein concentration of 2 mg/mL with lysis buffer.

3.9.2 SDS-PAGE

SDS-PAGE were sued to separate protein based on size under denaturating and reducing conditions. 25 µL of the IP samples, and 20 µL of the input and/or unbound was loaded on an 18-well 10% Bis-Tris gel (Bio-Rad, #567-1034). TGS running buffer (Appendix I - Solutions) and Benchmark protein ladder (Invitrogen, #10742-012) was used for identification of protein size.

3.9.3 Western Blotting

For Western blot analysis, nitrocellulose membranes were used (Bio-Rad, #170-4159). The protein content from the gel was transfered to the membrane using Trans Blot Turbo Transfer (Bio-Rad, #10022518). Next, the membrane was stained with Ponceau S Solution (Sigma-Aldrich, #SLBN3529V), revealing the Benchmarker for membrane cut. The membrane pieces were blocked for 1 hr at 37°C with blocking buffer (5% milk protein in TBST), followed by incubation with primary antibody diluted in blocking buffer ON at 4°C in a humid chamber 0. Membrane pieces were washed for 5 min five times in TBST before incubation with phosphatase-conjugated secondary antibody (Goat α-Rabbit (Sigma-Aldrich #P0447) or Goat α-Mouse (Sigma-Aldrich, #P0449), diluted 1:500 in blocking buffer for 1 hr at RT. Membranes were washed for 5 min five times and chemiluminescence was initiated by incubation in substrate (Thermo-Fisher, #32106).

3.10 NBCn1 C-tail FLAG contructs

To determine the RACK1 interaction domain, a series of C-tail deletions of NBCn1 (rat NBCn1-D) were designed: fulllength 1118-1254 (137 amino acids), 1118-1238 (122 amino acids), 1118-1158 (42 amino acids), and 1118-1140 (22 amino acids). Primers were designed according the In-Fusion HD Cloning Kit guidelines (Takara Bio, #121416) described in section 3.7.1. They are presented in **Table 1** (IAX-10-16). In-Fusion cloning was carried out as described in section 3.7.2, with the exception of pFLAG-CMV-2 linearization using restriction enzymes EcoRI-HF (NEB, #R0101S) and KpnI-HF (NEB, #R3142S) in CutSmart buffer provided with the enzymes. The constructs were then transiently transfected into 60-8% confluent HEK293 cells using Lipofectamine 3000 (Invitrogen, #L3000-015) in a 1:6 ratio DNA to Lipofectamine, and media was changed after 6 to avoid toxic effects. After 24 hrs, cells were subjected to co-IP as described in section 3.8 with FLAG-pulldown.

4 Results

4.1 NBCn1 membrane localization depends on cell confluence

Preliminary data from our lab, show that high confluence is important for NBCn1 membrane localization. For later investigation of the NBCn1 sorting pathway(s), I set up a prestudy to determine the cell density needed for membrane localization. MDCK-II cells were seeded for IF in a series of densities on coverslips and stained with NBCn1 primary antibody and rhodamine phalloidin, a F-actin probe conjugated with red flourescent dye, which can be used to outline the plasma membrane. In agreement with the findings of my colleagues, I found that fully confluent cells expressed more NBCn1 in the plasma membrane compared to non-confluent cells (n = 3) (**Figure 7**), confirming that NBCn1 membrane localization depends on cell confluence.

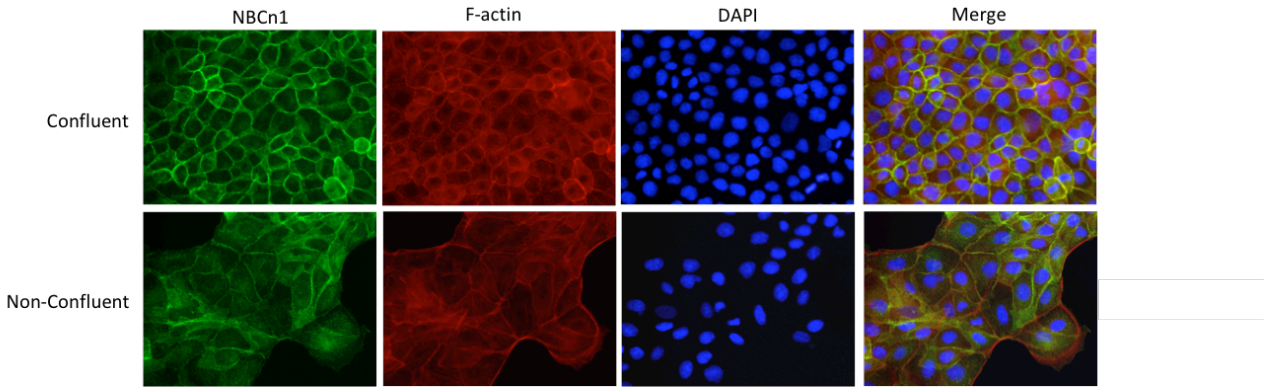

Figure 7 Example of NBCn1 localization in confluent versus non-confluent cells. Confluent cells were seeded with a density of $52 \cdot 10^3$ cells per cm^2, whereas the non-confluent were seeded with $16 \cdot 10^3$ cells per cm^2. Coverslips were stained with antibody against the N-terminal domain of NBCn1 (ntNBCn1), rhodamine phalloidin for F-actin, and DAPI for the nucleus.

4.2 NBCn1 trafficking to the membrane: A new pulse-chase approach is needed

Prior to the project, our lab created a C-terminally SNAP-and HA-tagged NBCn1 (rat NBCn1-D) in collaboration with Professor Michael Caplan from Yale Medical School, to study the trafficking pathway(s) of NBCn1 to the plasma membrane. SNAP-tagging is a great tool for protein trafficking analysis. It is based on the DNA-repair protein AGT, which reacts covalently with *O* ^{6}-benzylguanine (BG), resulting in transfer of the substituted benzyl group to the reactive thiol in the SNAP-tag (Stoops et al. 2014) (**Figure 8A**). Our lab has tested that the SNAP- and HA-tags do not affect the localization of NBCn1 (Olesen et al. 2018).

Most importantly, the SNAP-tag can be blocked, allowing pulse-chase experiments with the HA-tag as positive control. Unfortunately, a stable NBCn1-SNAP-HA-expressing cell line has not been possible to sustain in our lab as the cells tend to stop expressing the target gene, while still expressing the antibiotic resistance. To test the substrate-binding specificity and efficacy of BG-549 to the SNAP-tag, MDCK-II cells were transiently transfected with NBCn1-SNAP-HA. Cells were fixed and permeabilized before incubation in BG-549. Several experiments revealed what appeared to be nuclei staining with BG-549 (n = 3) (**Figure 8B**). To eliminate the possibility of nuclear membrane permeabilization and consequently accumulation of substrate inside the nucleus, substrate-binding experiments were carried on with another, permeable live-staining SNAP substrate, TMR-Star SNAP-Cell, with which we got rid of nuclei staining (n = 3) (**Figure 8C**). We later found that two DAPI-exciting diodes were on in the microscope, suggesting that the assumed nuclei staining was in fact, bleed-through from DAPI.

For pulse-chase experiments, the SNAP-tag reactivity was blocked using SNAP-Cell Block before incubation in TMR-Star SNAP-Cell. However, successfull blocking and live staining was only accomplished once (**Figure 8D**), as subsequent attempts of replication somehow resultet in unspecific staining of impurities (n = 3) (data not shown). To avoid this, and to accommodate the need for a stable cell line, lentiviral transduction was initiated as another pulse-chaise approach. NBCn1-SNAP-HA and N-terminally GFP-tagged NBCn1 (rat NBCn1-D) were respectively cloned into the lentiviral empty backbone plasmid pCW57.1 (Appendix II - Plasmids). Lentiviral transduction incorporates the target gene into the genome of the cells (Desfarges and Ciuffi 2010) and the pCW57.1 backbone, specifically, allows doxycyclin-inducible expression of the target gene by a system called tetracycline off. Tetracycline off is based on the fusion of the tet repressor (tetR), with the activating domain of viron protein 16 (VP16) of herpes simplex, resulting in a tetracycline-controlled transactivator (tTA) (Gossen and Bujard 1992). In the absence of tetracycline, the tetR part of the tTA will bind a tetracycline operator sequence and reduce the expression from it, while the VP16 promotes expression. Contrary, in the presents of tetracycline, tetracyclin binds the tetR part, enabling tTA-binding to the operator sequence, increasing target gene expression by the activation domain (Gossen and Bujard 1992). Thus, this transduction method would provide a stably expressed on/off system for transcription of GFP-NBCn1 and NBCn1-SNAP-HA in MDCK-II cells. Backbone contruct expression was validated in MCF-7 cells by IF analysis (data not shown). To produce backbone construct-expressing vira, HEK293T cells were transfected with backbone, pMD2.G (envelope), and pBR8.91 (packaging) plasmids, followed by virus harvest after two days. MDCK-II cells were incubated with virus for two days. Although this procedure was perfomed twice, no succesfull outcome was obtained and time constraints prevented further experiments by me. However, the work is continued in our

lab.

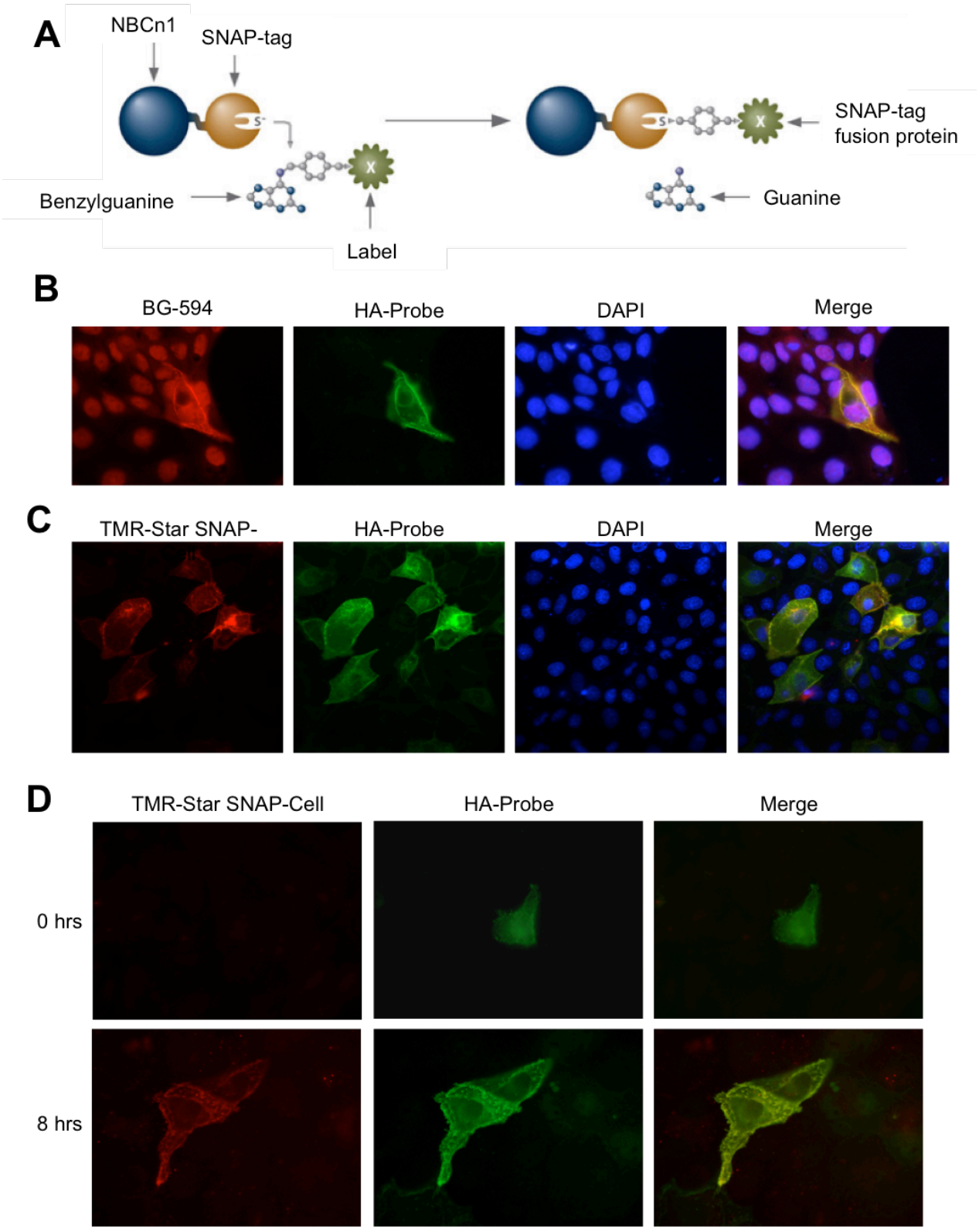
A
NBCn1
SNAP-tag
Benzylguanine
Label
SNAP-tag
fusion protein
Guanine
B
BG-594
HA-Probe
DAPI
Merge
C
TMR-Star SNAP-
HA-Probe
DAPI
Merge
D
TMR-Star SNAP-Cell
HA-Probe
Merge
0 hrs
8 hrs

Figure 8 SNAP-tag labeling experiments. A: The principle behind SNAP-tag labeling. See the text for more detailed description. **B**: Post-fixation SNAP-tag labeling with BG-549 in NBCn1-SNAP-HA transiently transfected MDCK-II cells. **C**: Live SNAP-tag labeling with TMR-Star SNAP-Cell in NBCn1-SNAP-HA transiently transfected MDCK-II cells. **D**: BG-block of SNAP-tag reactivity before live SNAP-tag labeling with TMR-Star SNAP-Cell in NBCn1-SNAP-HA transiently transfected MDCK-II cells.

4.3 NBCn1 trafficking to the plasma membrane via AP-1 clathrin-coated vesicles

We hypothesized that AP-1B clathrin-coated vesicles are responsible for the basolateral trafficking of NBCn1. To test this, non-confluent (70% confluency) and confluent MDCK-II cells were subjected to native co-IP. In congruence with our hypothesis, γ-adaptin was able to precipitate NBCn1 consistently in both confluent (n = 4) (**Figure 9B**) and non-confluent (n = 3) cells (**Figure 9A**), suggesting NBCn1 trafficking to the plasma membrane via AP-1 clathrin-coated vesicles.

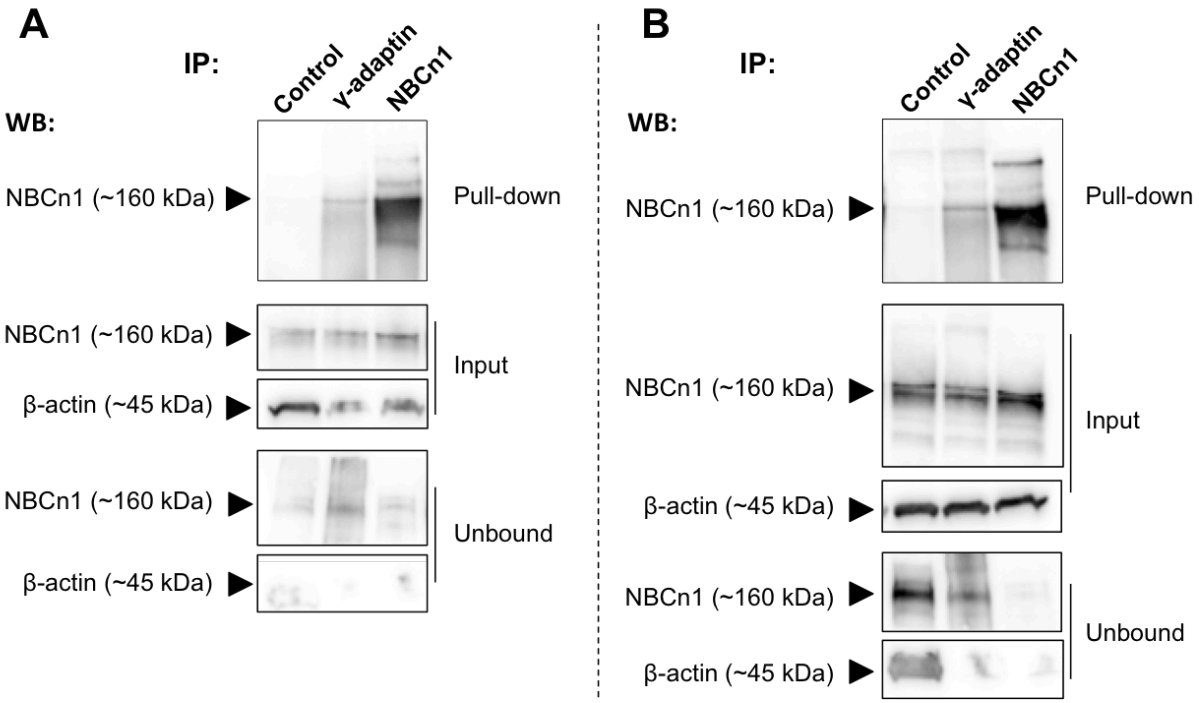

Figure 9 Co-IP of NBCn1 by γ-adaptin in MDCK-II cells. A: Co-IP in non-confluent cells (70% confluent). B: Co-IP in confluent cells. Under both conditions, γ –adaptin was able to precipitate NBCn1 to a greater extend than the IgG control.

4.4 RACK1 interacts with NBCn1 and is important for its membrane localization

Prior to this project, our lab demonstrated close proximity between RACK1 and NBCn1 in non-confluent MDCK-II and MCF-7 cells by *in situ* proximity ligase assay (PLA) (Olesen et al. 2018). PLA is a method an antibody-based method that can detect close intermolecular distance (< 40 nm) between two natively

expressed proteins (Pierre and Scholich 2010). To determine whether the close proximity was due to physical interaction between RACK1 and NBCn1, native co-IP was performed with non-confluent (70% confluence) and confluent MDCK-II cells, respectively, and with both proteins as bait. In non-confluent cells, NBCn1 was able to precipitate RACK1 (**Figure 10A**) and vice versa (**Figure 10B**), confirming physical interaction between the two (n = 4). Additionally, RACK1 was, in some cases, able to precipitate NBCn1 in confluent cells (data not shown). In this process, our lab also demonstrated reduced NBCn1 membrane expression in MCF-7 RACK1 KD cells, without altered overall NBCn1 expression (Olesen et al. 2018), indicating an important role for RACK1 in NBCn1 trafficking to the membrane.

To gain more knowledge of their interaction, we next asked which part of the NBCn1 C-tail interacted with RACK1. A truncation series of FLAG-tagged NBCn1 C-tail (rat NBCn1-D) was designed, spanning from the full length C-tail of 137 amino acids to the most proximal 22 amino acids. HEK293 cells were transfected with the different constructs and expression was validated by IF and WB for the FLAG protein (Olesen et al. 2018). Transfected HEK293 cells subjected to co-IP, followed by blotting for RACK1. All four constructs were able to precipitate RACK1 to a greater extent than the control transfections (sham, IgG control, and empty vector) (**Figure 10C**), suggesting that the most proximal 22 amino acids of the C-tail is sufficient for RACK1 interaction.

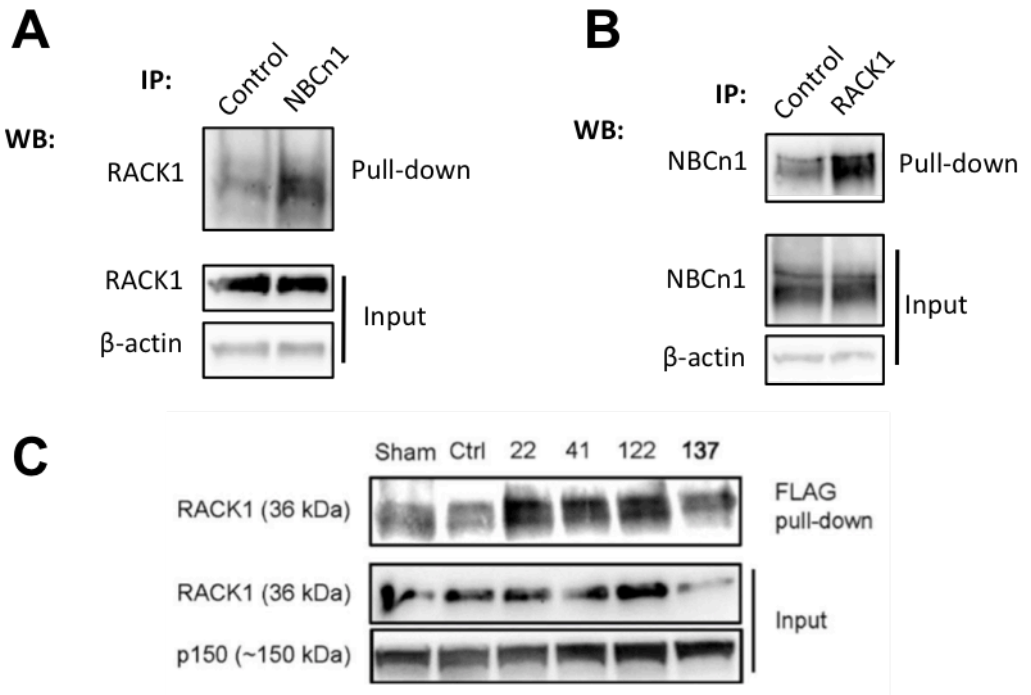

Figure 10 Co-IP of RACK1 and NBCn1 interaction. A: Co-IP in non-confluent cells (70% confluence) MDCK-II cells. NBCn1 is able to precipitate RACK1. **B**: RACK1 is able to precipitate NBCn1 under the same conditions. **C**: All NBCn1 truncations were able to precipitate RACK1, indicating that the most poximal 22 amino acids are sufficient for RACK1 interaction. Source: (Olesen et al. 2018). All figures are made in collaboration with Mark Severin and Dn Ploug Christensen.

4.5 NBCn1 interacts with lateral polarity proteins in MDCK-II cells

NBCn1 localizes to the basolateral membrane most epithelial cells (Damkier, Nielsen, and Praetorius 2006). By confocal microscopy, our lab has found both endogenous NBCn1 and exogenous GFP-NBCn1 (rat NBCn1-D with GFP-coupled N-terminus) consistently localized in the basolateral membrane of polarized MDCK-II cells (Olesen et al. 2018). Interestingly, in the GFP-NBCn1-expressing cells grown on transfilters, NBCn1 seems to be predominantly localized in the lateral membrane rather than distributed evenly in the basolateral membrane (Olesen et al. 2018). Relevant for this localization, the MS analysis suggested several lateral interaction candidates, such as Claudin 3, LLGL-1, DLG, and Scribble (Olesen et al. 2018). To investigate the potential physical interaction between NBCn1 and these putative interactors, MDCK-II cells were seeded in 100 mm dishes and allowed to polarize for 9 days prior to native co-IP. In coherence with this (baso)lateral expression, LLGL-1 was consistently able to precipitate endogenous NBCn1 (n = 3) (**Figure 11**), suggesting physical interaction between the two proteins. Additionally, another Scribble complex component DLG (SAP97) was able to precipitate NBCn1 (n = 2). However, the Scribble protein was not able to precipitate NBCn1 to a greater extent than the IgG control in these experiments (**Figure 11**). The same was true for Claudin 3 in most experiments, although it was able to precipitate NBCn1 in one case (**Figure 11**). The scaffold protein cortactin was not able to precipitate in these experiments (n = 2) (**Figure 12**).

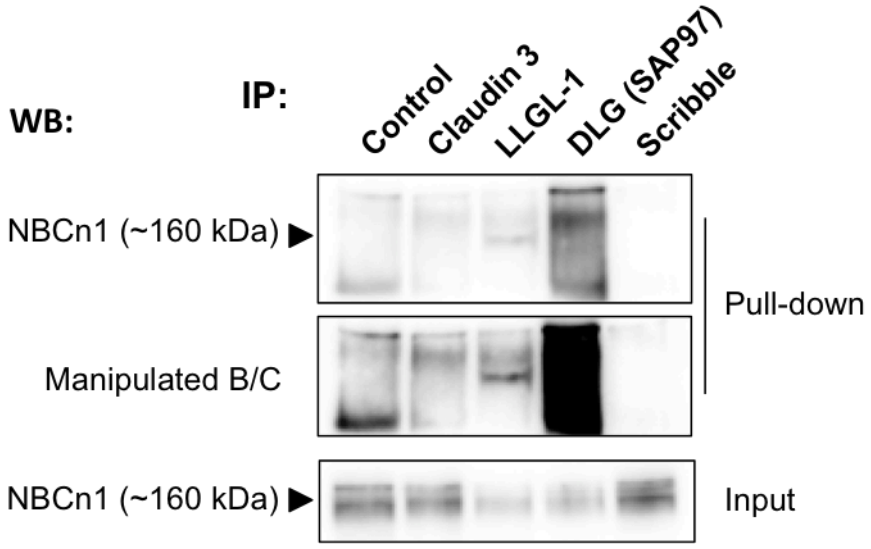

Figure 11 Co-IP of NBCn1 LLGL-1 and DLG in MDCK-II cells. Both LLGL-1 and DLG were able to precipitate NBCn1 in polarized MDCK-II cells. Possibly also Claudin 3, although validation is needed. Scribble was, however, not able to pull-down NBCn1 in these experiments.

4.6 Screening for potetial interaction partners in polarized cells

To investigate the trafficking pathway(s) of NBCn1 in polarized epithelial cells, we set up co-IP screening experiment. For early endsome-association Rab4 and Rab5 were taken into account. For late endosome-association, Rab7 was selected. For recycling endosome-associtaion Rab11, and Rab10 is involved in the basolateral sorting in epithelial cells (data not shown). Early endosome-associated Rab4 showed a slight pull-down of NBCn1 and further investigation is needed for confirmation (n =2). However, none of the other Rab GTPases were able to pull-down NBCn1 in this work (n=2) **Figure 12**. The same was true for retromer components SNX27 and VPS35 **Figure 12** and lysosomal-associated membrane protein 1 (LAMP-1).

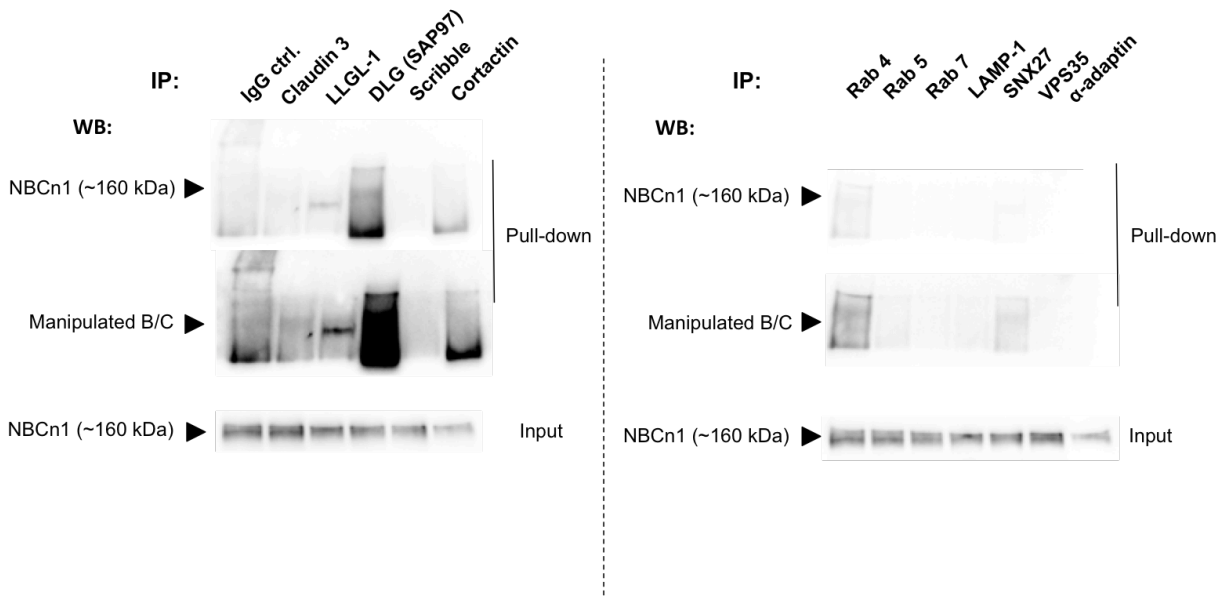

Figure 12 Co-IP Screening for NBCn1 interactors in polarized in MDCK-II cells. LLGL-1 and DLG are clearly able to precipitate NBCn1, whereas Claudin 3, Rab4 and SNX27 are able to pull-down NBCn1 to more or less the same extent as the IgG control.

5 Discussion

Despite the well describes importance of NBCn1 in physiology (Boedtkjer, Bunch, and Pedersen 2012) and several diaseases, including breast cancer (Boedtkjer et al. 2013, Lee et al. 2015), there was, when I started this project, a near-complete lack of knowledge regarding the sorting, trafficking and turnover of NBCn1 in epithelial cells.

In epithelial cells, such as the renal medullary and duodenum epithelia, NBCn1 localizes to the basolateral membrane (Damkier, Nielsen, and Praetorius 2006, Olesen et al. 2018), with the exception of the choroid plexus epithelium (Praetorius and Nielsen 2006). The cytosolic C-tail of NBCn1 contains a PDZ-binding domain in the most distal part. Deletion of the C-tail, but not the PDZ domain alone, abolishes the membrane localization (Loiselle, Jaschke, and Casey 2003, Olesen et al. 2018, Arakawa et al. 2015). In MDCK-II cells grown on Transwell filters, a more lateral NBCn1 localization has been seen compared to other basolateral transporters (Olesen et al. 2018). In congruence with this, MS analyses by our lab suggest lateral interaction partners, such as Claudin 3, LLGL-1, DLG, and Scribble (Olesen et al. 2018). In this work, co-IP suggested physical interaction between endogenous NBCn1 and the lateral protein LLGL-1 and DLG, which could contribute to a more lateral localization of NBCn1. However, polarized MDCK-II cells transiently transfected with GFP-NBCn1 (rat NBCn1-D) show a more evenly distributed basolateral localization (Olesen et al. 2018), suggesting that either the NBCn1 variants differ in their targeting pattern or, perhaps more likely, imaging of basolateral membrane is hindered when cells are grown on Transwell filters.

The trafficking of many basolateral membrane proteins involves the epithelial-specific AP-1B complex (Fölsch et al. 1999, Gan, McGraw, and Rodriguez-Boulan 2002), yet not all epithelial cells express AP-1B and AP-4 may also play a role (Simmen et al. 2002, Fölsch 2005). In congruence with this, endogenous NBCn1 interaction with the AP-1 γ-component was found in this project, suggesting AP-1 clathrin-coated vesicle transport of NBCn1 to the plasma membrane, possibly through binding to a non-canonical sorting motif. However, this finding does not reveal the trafficking pathway from ER to the membrane, which can be either directly or through recycling endsomes (Duffield, Caplan, and Muth 2008). In this project, none of the GTPases tested were not able to precipitate NBCn1, except for maybe Rab4. However, co-IP has the disadvantage of being dependent on the ability of an antibody to specifically and stably bind the bait protein, optimization of the procedure or other approaches are needed to determine the interactors of NBCn1.

One major finding for the trafficking of NBCn1 to the membrane, is its interaction with scaffold protein RACK1. This is supported by the reciprocal precipitation of endogenous NBCn1 and RACK1, *in*

situ PLA and pulldown of RACK1 with FLAG-tagged NBCn1 C-tail constructs, in which the most proximal 22 amino acids were sufficient for RACK1 interaction (Olesen et al. 2018). Furthermore our lab has shown, that RACK1 KD reduces the NBCn1 localization without changing the total expression of NBCn1 and that one third of NBCn1 is constitutively endosytosed (Olesen et al. 2018), suggesting NBCn1 recycling between the basolateral membrane and other intracellular compartments. This would be in agreement with the findings of weak pull-down of NBCn1 by early endosome-associated Rab4. Notably, this needs confirmation through futher studies.

6 Conclusion

This project contributes to a greater understanding of the trafficking pathway(s) of newly synthesized NBCn1. Co-IP experiments revealed interation between endogenous NBCn1 and the AP-1 component γ-adaptin, suggesting that NBCn1 is sorted to the membrane via AP-1 clathrin coated vesicles. In congruence with the basolateral localization of NBCn1, another great finding by co-IP, was the interaction between endogenous NBCn1 and the lateral polarity protein complex components LLGL-1 and DLG, indicating their role in NBCn1 localization. Lastely, a key finding in this work is the interaction between scaffolding protein RACK1 and NBCn1, which support the findings of our lab that RACK1 is important for the membrane sorting of NBCn1. Furthermore, truncations of the NBCn1 C-tail were able to pull-down RACK1, implicating that the proximal 22 amino acids are sufficient for RACK1 interaction.

Appendix I - Solutions

6.1.1 Phosphate-buffered saline (PBS)

NaCl (136.89 mM)

KCl (2.68 mM)

$Na_2HPO_4 – 2\ H_2O$ (8.1 mM)

KH_2PO_4 (1.47 mM)

Diluted in ddH_2O and pH adjusted to 7.4 with NaOH/HCl. Autoclaved

6.1.2 Trypsin Mix (2x)

Trypsin-EDTA (10x) (Invitrogen, Gibco, # 15400-054)

PBS

6.1.3 TBST (Tris-Buffered Saline Tween 20)

10 mM Tris/Hcl

120 mM NaCl

0.1% TWEEN 20

Dissolved in ddH_2O

6.1.4 TGS (Tris/Glycine/SDS) running buffer

Tris/Glycine/SDS (125 mM Trism, 192 mM glycine, 0.1% SDS, pH 8.3, BioRad, #161-0732) diluted ten times in ddH_2O.

Appendix II - Plasmids

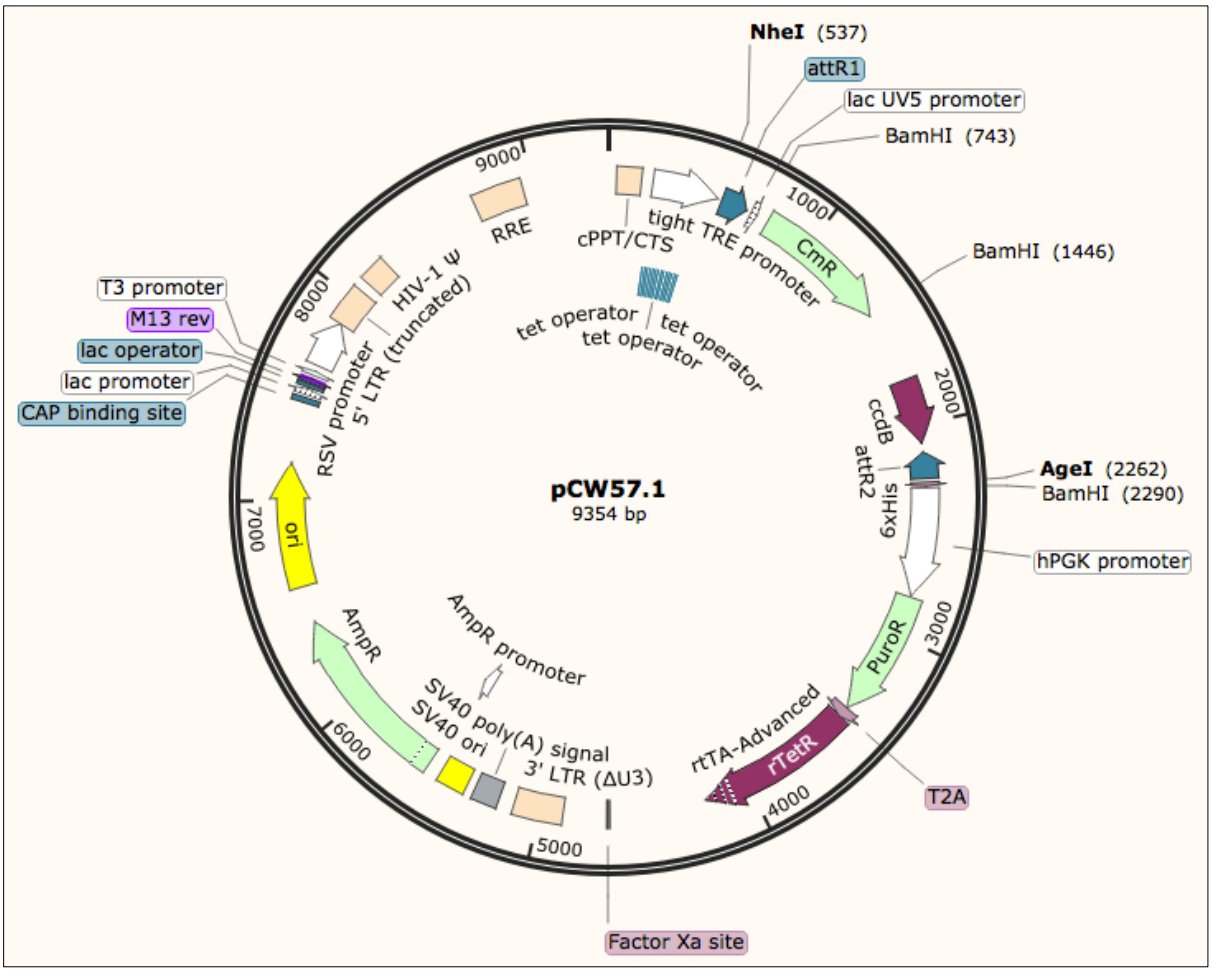

Figure 13. The 3rd generation lentiviral transfer plasmid pCW57.1. For In-Fusion cloning, the expression vector was linearized by NheI and AgeI restriction enzyme digestion. Cutting out the ccDB gene is a positive selection method as the CcdB protein induces gyrase clavage of DNA and thereby cell death. DNA breakage occours when CcdB traps gyrase covalently attached to DNA in the intermediate complex between transient breakage in DNA, passing a DNA segment through the brak, and resealing the break during transcription or replication (Bernard et al. 1993).

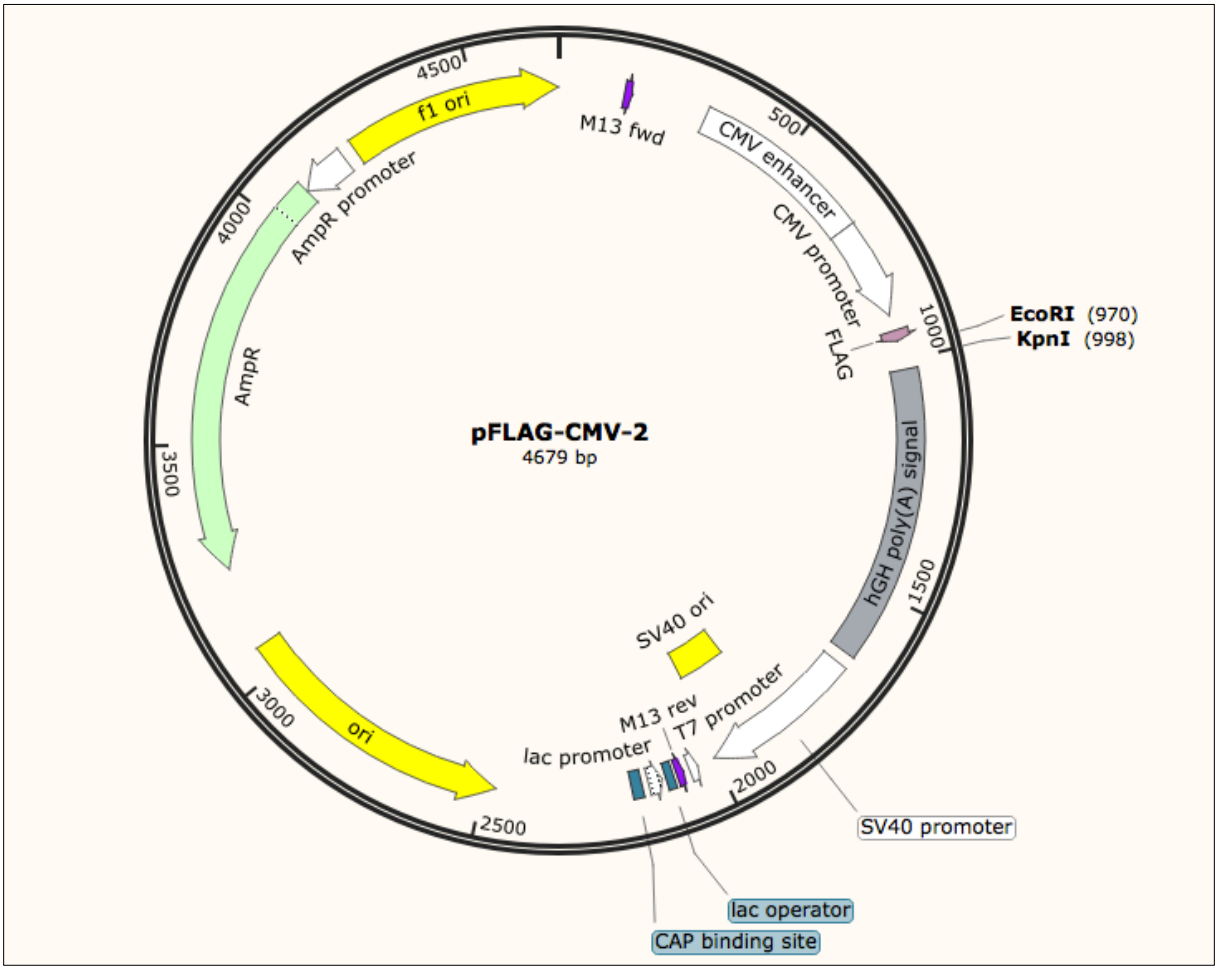

Figure 14. The FLAG expression vector used for FLAG-tagged NBCn1 c-terminus truncations. For In-Fusion cloning, pFLAG-CMV was linearized by double digestion with EcoRI and KpnI.

Appendix III - Primers

Primer name	T_m	Difference	CG%	Self-compl.	Last five
IAX-FWD-1	64.21°C	1.47°C	72.11%	4.00	GGGCC
IAX-REV-2	62.74°C		48.00%	0.00	TGGGG
IAX-FWD-5	59.73°C	1.35°C	61.11%	0.00	GCCAG
IAX-REV-6	58.38°C		36.00%	4.00	CCATG
IAX-FWD-10	57.82°C		43.48%	1.00	TAGTC
IAX-REV-12	56.34°C		40.91%	1.00	TGAGG

IAX-REV-13	57.03°C	41.67%	0.00	TCATC
IAX-REV-14	59.60°C	50.00%	0.00	CATTT
IAX-REV-15	57.75°C	32.00%	3.00	TCGAA
IAX-REV-16	56.29°C	40.91%	4.00	CCATG

Table 4. 3' end properties of primers used to clone NBCn1-GFP (IAX-FWD-5 and IAX-REV-6) or NBCn1-SNAP-HA (IAX-FWD-1 and IAX-REV-2) into the lentiviral transfer plasmid pCW57.1. Deviations from the IN-Fusion Cloning Kit guidelines (Takara Bio, #121416) are marked in red.

7 References

Aalkjaer, C., E. Boedtkjer, I. Choi, and S. Lee. 2014. "Cation-coupled bicarbonate transporters." *Compr Physiol* 4 (4):1605-37. doi: 10.1002/cphy.c130005.

Andersen, A. P., M. Flinck, E. K. Oernbo, N. B. Pedersen, B. M. Viuff, and S. F. Pedersen. 2016. "Roles of acid-extruding ion transporters in regulation of breast cancer cell growth in a 3-dimensional microenvironment." *Mol Cancer* 15 (1):45. doi: 10.1186/s12943-016-0528-0.

Andersen, A. P., J. Samsøe-Petersen, E. K. Oernbo, E. Boedtkjer, J. M. A. Moreira, M. Kveiborg, and S. F. Pedersen. 2018. "The net acid extruders NHE1, NBCn1 and MCT4 promote mammary tumor growth through distinct but overlapping mechanisms." *Int J Cancer* 142 (12):2529-2542. doi: 10.1002/ijc.31276.

Ang, A. L., T. Taguchi, S. Francis, H. Fölsch, L. J. Murrells, M. Pypaert, G. Warren, and I. Mellman. 2004. "Recycling endosomes can serve as intermediates during transport from the Golgi to the plasma membrane of MDCK cells." *J Cell Biol* 167 (3):531-43. doi: 10.1083/jcb.200408165.

Arakawa, T., T. Kobayashi-Yurugi, Y. Alguel, H. Iwanari, H. Hatae, M. Iwata, Y. Abe, T. Hino, C. Ikeda-Suno, H. Kuma, D. Kang, T. Murata, T. Hamakubo, A. D. Cameron, T. Kobayashi, N. Hamasaki, and S. Iwata. 2015. "Crystal structure of the anion exchanger domain of human erythrocyte band 3." *Science* 350 (6261):680-4. doi: 10.1126/science.aaa4335.

ATCC. "293T (ATCC ® CRL-3216 ™)." accessed 16th of April. https://www.lgcstandards-atcc.org/products/all/CRL-3216.aspx?geo_country=dk - characteristics.

Bernard, P., K. E. Kézdy, L. Van Melderen, J. Steyaert, L. Wyns, M. L. Pato, P. N. Higgins, and M. Couturier. 1993. "The F plasmid CcdB protein induces efficient ATP-dependent DNA cleavage by gyrase." *J Mol Biol* 234 (3):534-41. doi: 10.1006/jmbi.1993.1609.

Bilder, D., M. Schober, and N. Perrimon. 2003. "Integrated activity of PDZ protein complexes regulates epithelial polarity." *Nat Cell Biol* 5 (1):53-8. doi: 10.1038/ncb897.

Boedtkjer, E., L. Bunch, and S. F. Pedersen. 2012. "Physiology, pharmacology and pathophysiology of the pH regulatory transport proteins NHE1 and NBCn1: similarities, differences, and implications for cancer therapy." *Curr Pharm Des* 18 (10):1345-71.

Boedtkjer, E., J. M. Moreira, M. Mele, P. Vahl, V. T. Wielenga, P. M. Christiansen, V. E. Jensen, S. F. Pedersen, and C. Aalkjaer. 2013. "Contribution of Na+,HCO3(-)-cotransport to cellular pH control in human breast cancer: a role for the breast cancer susceptibility locus NBCn1 (SLC4A7)." *Int J Cancer* 132 (6):1288-99. doi: 10.1002/ijc.27782.

Boedtkjer, E., J. Praetorius, V. V. Matchkov, E. Stankevicius, S. Mogensen, A. C. Füchtbauer, U. Simonsen, E. M. Füchtbauer, and C. Aalkjaer. 2011. "Disruption of Na+,HCO_3^- cotransporter NBCn1 (slc4a7) inhibits NO-mediated vasorelaxation, smooth muscle Ca^{2+} sensitivity, and hypertension development in mice." *Circulation* 124 (17):1819-29. doi: 10.1161/CIRCULATIONAHA.110.015974.

Bok, D., G. Galbraith, I. Lopez, M. Woodruff, S. Nusinowitz, H. BeltrandelRio, W. Huang, S. Zhao, R. Geske, C. Montgomery, I. Van Sligtenhorst, C. Friddle, K. Platt, M. J. Sparks, A. Pushkin, N. Abuladze, A. Ishiyama, R. Dukkipati, W. Liu, and I. Kurtz. 2003. "Blindness and auditory impairment caused by loss of the sodium bicarbonate cotransporter NBC3." *Nat Genet* 34 (3):313-9. doi: 10.1038/ng1176.

Chen, M., J. Praetorius, W. Zheng, F. Xiao, B. Riederer, A. K. Singh, N. Stieger, J. Wang, G. E. Shull, C. Aalkjaer, and U. Seidler. 2012. "The electroneutral Na^+:HCO_3^- cotransporter NBCn1 is a major pHi regulator in murine duodenum." *J Physiol* 590 (14):3317-33. doi: 10.1113/jphysiol.2011.226506.

Chen, W., R. Zhong, J. Ming, L. Zou, B. Zhu, X. Lu, J. Ke, Y. Zhang, L. Liu, X. Miao, and T. Huang. 2012. "The SLC4A7 variant rs4973768 is associated with breast cancer risk: evidence from a case-control study and a meta-analysis." *Breast Cancer Res Treat* 136 (3):847-57. doi: 10.1007/s10549-012-2309-9.

Choi, I., C. Aalkjaer, E. L. Boulpaep, and W. F. Boron. 2000. "An electroneutral sodium/bicarbonate cotransporter NBCn1 and associated sodium channel." *Nature* 405 (6786):571-5. doi: 10.1038/35014615.

César-Razquin, A., B. Snijder, T. Frappier-Brinton, R. Isserlin, G. Gyimesi, X. Bai, R. A. Reithmeier, D. Hepworth, M. A. Hediger, A. M. Edwards, and G. Superti-Furga. 2015. "A Call for Systematic Research on Solute Carriers." *Cell* 162 (3):478-87. doi: 10.1016/j.cell.2015.07.022.

Damkier, H. H., S. Nielsen, and J. Praetorius. 2006. "An anti-NH2-terminal antibody localizes NBCn1 to heart endothelia and skeletal and vascular smooth muscle cells." *Am J Physiol Heart Circ Physiol* 290 (1):H172-80. doi: 10.1152/ajpheart.00713.2005.

Danielsen, A. A., M. D. Parker, S. Lee, W. F. Boron, C. Aalkjaer, and E. Boedtkjer. 2013. "Splice cassette II of Na+,HCO3(-) cotransporter NBCn1 (slc4a7) interacts with calcineurin A: implications for transporter activity and intracellular pH control during rat artery contractions." *J Biol Chem* 288 (12):8146-55. doi: 10.1074/jbc.M113.455386.

Day, C. A., N. W. Baetz, C. A. Copeland, L. J. Kraft, B. Han, A. Tiwari, K. R. Drake, H. De Luca, D. J. Chinnapen, M. W. Davidson, R. K. Holmes, M. G. Jobling, T. A. Schroer, W. I. Lencer, and A. K. Kenworthy. 2015. "Microtubule motors power plasma membrane tubulation in clathrin-independent endocytosis." *Traffic* 16 (6):572-90. doi: 10.1111/tra.12269.

Desfarges, S., and A. Ciuffi. 2010. "Retroviral integration site selection." *Viruses* 2 (1):111-30. doi: 10.3390/v2010111.

Duffield, A., M. J. Caplan, and T. R. Muth. 2008. "Protein trafficking in polarized cells." *Int Rev Cell Mol Biol* 270:145-79. doi: 10.1016/S1937-6448(08)01404-4.

Ehret, G. B., P. B. Munroe, K. M. Rice, M. Bochud, A. D. Johnson, D. I. Chasman, A. V. Smith, M. D. Tobin, G. C. Verwoert, S. J. Hwang, V. Pihur, P. Vollenweider, P. F. O'Reilly, N. Amin, J. L. Bragg-Gresham, A. Teumer, N. L. Glazer, L. Launer, J. H. Zhao, Y. Aulchenko, S. Heath, S. Sõber, A. Parsa, J. Luan, P. Arora, A. Dehghan, F. Zhang, G. Lucas, A. A. Hicks, A. U. Jackson, J. F. Peden, T. Tanaka, S. H. Wild, I. Rudan, W. Igl, Y. Milaneschi, A. N. Parker, C. Fava, J. C. Chambers, E. R. Fox, M. Kumari, M. J. Go, P. van der Harst, W. H. Kao, M. Sjögren, D. G. Vinay, M. Alexander, Y. Tabara, S. Shaw-Hawkins, P. H. Whincup, Y. Liu, G. Shi, J. Kuusisto, B. Tayo, M. Seielstad, X. Sim, K. D. Nguyen, T. Lehtimäki, G. Matullo, Y. Wu, T. R. Gaunt, N. C. Onland-Moret, M. N. Cooper, C. G. Platou, E. Org, R. Hardy, S. Dahgam, J. Palmen, V. Vitart, P. S. Braund, T. Kuznetsova, C. S. Uiterwaal, A. Adeyemo, W. Palmas, H. Campbell, B. Ludwig, M. Tomaszewski, I. Tzoulaki, N. D. Palmer, T. Aspelund, M. Garcia, Y. P. Chang, J. R. O'Connell, N. I. Steinle, D. E. Grobbee, D. E. Arking, S. L. Kardia, A. C. Morrison, D. Hernandez, S. Najjar, W. L. McArdle, D. Hadley, M. J. Brown, J. M. Connell, A. D. Hingorani, I. N. Day, D. A. Lawlor, J. P. Beilby, R. W. Lawrence, R. Clarke, J. C. Hopewell, H. Ongen, A. W. Dreisbach, Y. Li, J. H. Young, J. C. Bis, M. Kähönen, J. Viikari, L. S. Adair, N. R. Lee, M. H. Chen, M. Olden, C. Pattaro, J. A. Bolton, A. Köttgen, S. Bergmann, V. Mooser, N. Chaturvedi, T. M. Frayling, M. Islam, T. H. Jafar, J. Erdmann, S. R. Kulkarni, S. R. Bornstein, J. Grässler, L. Groop, B. F. Voight, J. Kettunen, P. Howard, A. Taylor, S. Guarrera, F. Ricceri, V. Emilsson, A. Plump, I. Barroso, K. T. Khaw, A. B. Weder, S. C. Hunt, Y. V. Sun, R. N. Bergman, F. S. Collins, L. L. Bonnycastle, L. J. Scott, H. M. Stringham, L. Peltonen, M. Perola, E. Vartiainen, S. M. Brand, J. A. Staessen, T. J. Wang, P. R. Burton, M. Soler Artigas, Y. Dong, H. Snieder, X. Wang, H. Zhu, K. K. Lohman, M. E. Rudock, S. R. Heckbert, N. L. Smith, K. L. Wiggins, A. Doumatey, D. Shriner, G. Veldre, M. Viigimaa, S. Kinra, D. Prabhakaran, V. Tripathy, C. D. Langefeld, A. Rosengren, D. S. Thelle, A. M. Corsi, A. Singleton, T. Forrester, G. Hilton, C. A. McKenzie, T. Salako, N. Iwai, Y. Kita, T. Ogihara, T. Ohkubo, T. Okamura, H. Ueshima, S. Umemura, S. Eyheramendy, T. Meitinger, H. E. Wichmann, Y. S. Cho, H. L. Kim, J. Y. Lee, J. Scott, J. S. Sehmi, W. Zhang, B. Hedblad, P. Nilsson, G. D. Smith, A. Wong, N. Narisu, A. Stančáková, L. J. Raffel, J. Yao, S. Kathiresan, C. J. O'Donnell, S. M. Schwartz, M. A. Ikram, W. T. Longstreth, T. H. Mosley, S. Seshadri, N. R. Shrine, L. V. Wain, M. A. Morken, A. J. Swift, J. Laitinen, I. Prokopenko, P. Zitting, J. A. Cooper, S. E. Humphries, J. Danesh, A. Rasheed, A. Goel, A. Hamsten, H. Watkins, S. J. Bakker, W. H. van Gilst, C. S. Janipalli, K. R. Mani, C. S. Yajnik, A. Hofman, F. U. Mattace-Raso, B. A. Oostra, A. Demirkan, A. Isaacs, F. Rivadeneira, E. G. Lakatta, M. Orru, A. Scuteri, M. Ala-Korpela, A. J. Kangas, L. P. Lyytikäinen, P. Soininen, T. Tukiainen, P. Würtz, R. T. Ong, M. Dörr, H. K. Kroemer, U. Völker, H. Völzke, P. Galan, S. Hercberg, M. Lathrop, D. Zelenika, P. Deloukas, M. Mangino, T. D. Spector, G. Zhai, J. F. Meschia, M. A. Nalls, P. Sharma, J. Terzic, M. V. Kumar, M. Denniff, E. Zukowska-Szczechowska, L. E. Wagenknecht, F. G. Fowkes, F. J. Charchar, P. E. Schwarz, C. Hayward, X. Guo, C. Rotimi, M. L. Bots, E. Brand, N. J. Samani, O. Polasek, P. J. Talmud, F. Nyberg, D. Kuh, M. Laan, K. Hveem, L. J. Palmer, Y. T. van der Schouw, J. P. Casas, K. L. Mohlke, P. Vineis, O. Raitakari, S. K. Ganesh, T. Y. Wong, E. S. Tai, R. S. Cooper, M. Laakso, D. C. Rao, T. B. Harris, R. W. Morris, A. F. Dominiczak, M. Kivimaki, M. G. Marmot, T. Miki, D. Saleheen, G. R. Chandak, J. Coresh, G. Navis, V. Salomaa, B. G. Han, X. Zhu, J. S. Kooner, O. Melander, P. M. Ridker, S. Bandinelli, U. B. Gyllensten, A. F. Wright, J. F. Wilson, L. Ferrucci, M. Farrall, J. Tuomilehto, P. P. Pramstaller, R. Elosua, N. Soranzo, E. J. Sijbrands, D. Altshuler, R. J. Loos, A. R. Shuldiner, C. Gieger, P. Meneton, A. G. Uitterlinden, N. J. Wareham, V. Gudnason, J. I. Rotter, R. Rettig, M. Uda, D. P. Strachan, J. C. Witteman, A. L. Hartikainen, J. S. Beckmann, E. Boerwinkle, R. S. Vasan, M. Boehnke, M. G. Larson, M. R. Järvelin, B. M. Psaty, G. R. Abecasis, A. Chakravarti, P. Elliott, C. M. van Duijn, C. Newton-Cheh, D. Levy, M. J. Caulfield, T. Johnson, International Consortium for Blood Pressure Genome-Wide Association Studies, CARDIoGRAM consortium, CKDGen Consortium, KidneyGen Consortium, EchoGen consortium, and CHARGE-HF consortium. 2011. "Genetic variants in novel pathways influence blood pressure and cardiovascular disease risk." *Nature* 478 (7367):103-9. doi: 10.1038/nature10405.

Farr, G. A., M. Hull, I. Mellman, and M. J. Caplan. 2009. "Membrane proteins follow multiple pathways to the basolateral cell surface in polarized epithelial cells." *J Cell Biol* 186 (2):269-82. doi: 10.1083/jcb.200901021.

Flinck, M., S. H. Kramer, and S. F. Pedersen. 2018. "Roles of pH in control of cell proliferation." *Acta Physiol (Oxf)*:e13068. doi: 10.1111/apha.13068.

Fölsch, H. 2005. "The building blocks for basolateral vesicles in polarized epithelial cells." *Trends Cell Biol* 15 (4):222-8. doi: 10.1016/j.tcb.2005.02.006.

Fölsch, H., H. Ohno, J. S. Bonifacino, and I. Mellman. 1999. "A novel clathrin adaptor complex mediates basolateral targeting in polarized epithelial cells." *Cell* 99 (2):189-98.

Gan, Y., T. E. McGraw, and E. Rodriguez-Boulan. 2002. "The epithelial-specific adaptor AP1B mediates post-endocytic recycling to the basolateral membrane." *Nat Cell Biol* 4 (8):605-9. doi: 10.1038/ncb827.

Gorbatenko, A., C. W. Olesen, N. Mørup, G. Thiel, T. Kallunki, E. Valen, and S. F. Pedersen. 2014. "ErbB2 upregulates the Na+,HCO3(-)-cotransporter NBCn1/SLC4A7 in human breast cancer cells via Akt, ERK, Src, and Kruppel-like factor 4." *FASEB J* 28 (1):350-63. doi: 10.1096/fj.13-233288.

Gossen, M., and H. Bujard. 1992. "Tight control of gene expression in mammalian cells by tetracycline-responsive promoters." *Proc Natl Acad Sci U S A* 89 (12):5547-51.

Graham, F. L., J. Smiley, W. C. Russell, and R. Nairn. 1977. "Characteristics of a human cell line transformed by DNA from human adenovirus type 5." *J Gen Virol* 36 (1):59-74. doi: 10.1099/0022-1317-36-1-59.

Grindstaff, K. K., C. Yeaman, N. Anandasabapathy, S. C. Hsu, E. Rodriguez-Boulan, R. H. Scheller, and W. J. Nelson. 1998. "Sec6/8 complex is recruited to cell-cell contacts and specifies transport vesicle delivery to the basal-lateral membrane in epithelial cells." *Cell* 93 (5):731-40.

Hall, H. G., D. A. Farson, and M. J. Bissell. 1982. "Lumen formation by epithelial cell lines in response to collagen overlay: a morphogenetic model in culture." *Proc Natl Acad Sci U S A* 79 (15):4672-6.

Hanahan, D., and R. A. Weinberg. 2011. "Hallmarks of cancer: the next generation." *Cell* 144 (5):646-74. doi: 10.1016/j.cell.2011.02.013.

Herrmann, S., M. Ninkovic, T. Kohl, É Lörinczi, and L. A. Pardo. 2012. "Cortactin controls surface expression of the voltage-gated potassium channel K(V)10.1." *J Biol Chem* 287 (53):44151-63. doi: 10.1074/jbc.M112.372540.

Iden, S., and J. G. Collard. 2008. "Crosstalk between small GTPases and polarity proteins in cell polarization." *Nat Rev Mol Cell Biol* 9 (11):846-59. doi: 10.1038/nrm2521.

Jahn, R., and R. H. Scheller. 2006. "SNAREs--engines for membrane fusion." *Nat Rev Mol Cell Biol* 7 (9):631-43. doi: 10.1038/nrm2002.

Kang, R. S., and H. Fölsch. 2009. "An old dog learns new tricks: novel functions of the exocyst complex in polarized epithelia in animals." *F1000 Biol Rep* 1:83. doi: 10.3410/B1-83.

Lauritzen, G., M. B. Jensen, E. Boedtkjer, R. Dybboe, C. Aalkjaer, J. Nylandsted, and S. F. Pedersen. 2010. "NBCn1 and NHE1 expression and activity in DeltaNErbB2 receptor-expressing MCF-7 breast cancer cells: contributions to pHi regulation and chemotherapy resistance." *Exp Cell Res* 316 (15):2538-53. doi: 10.1016/j.yexcr.2010.06.005.

Lee, S., M. Mele, P. Vahl, P. M. Christiansen, V. E. Jensen, and E. Boedtkjer. 2015. "Na+,HCO3- -cotransport is functionally upregulated during human breast carcinogenesis and required for the inverted pH gradient across the plasma membrane." *Pflugers Arch* 467 (2):367-77. doi: 10.1007/s00424-014-1524-0.

Loiselle, F. B., P. Jaschke, and J. R. Casey. 2003. "Structural and functional characterization of the human NBC3 sodium/bicarbonate co-transporter carboxyl-terminal cytoplasmic domain." *Mol Membr Biol* 20 (4):307-17. doi: 10.1080/0968768031000122520.

Mayor, S., and R. E. Pagano. 2007. "Pathways of clathrin-independent endocytosis." *Nat Rev Mol Cell Biol* 8 (8):603-12. doi: 10.1038/nrm2216.

McMahon, H. T., and E. Boucrot. 2011. "Molecular mechanism and physiological functions of clathrin-mediated endocytosis." *Nat Rev Mol Cell Biol* 12 (8):517-33. doi: 10.1038/nrm3151.

Mellman, I., and W. J. Nelson. 2008. "Coordinated protein sorting, targeting and distribution in polarized cells." *Nat Rev Mol Cell Biol* 9 (11):833-45. doi: 10.1038/nrm2525.

Moskalenko, S., D. O. Henry, C. Rosse, G. Mirey, J. H. Camonis, and M. A. White. 2002. "The exocyst is a Ral effector complex." *Nat Cell Biol* 4 (1):66-72. doi: 10.1038/ncb728.

Müsch, A., D. Cohen, C. Yeaman, W. J. Nelson, E. Rodriguez-Boulan, and P. J. Brennwald. 2002. "Mammalian homolog of Drosophila tumor suppressor lethal (2) giant larvae interacts with basolateral exocytic machinery in Madin-Darby canine kidney cells." *Mol Biol Cell* 13 (1):158-68. doi: 10.1091/mbc.01-10-0496.

Nejsum, L. N., and W. J. Nelson. 2009. "Epithelial cell surface polarity: the early steps." *Front Biosci (Landmark Ed)* 14:1088-98.

Odgaard, E., J. K. Jakobsen, S. Frische, J. Praetorius, S. Nielsen, C. Aalkjaer, and J. Leipziger. 2004. "Basolateral Na+-dependent HCO3- transporter NBCn1-mediated HCO3- influx in rat medullary thick ascending limb." *J Physiol* 555 (Pt 1):205-18. doi: 10.1113/jphysiol.2003.046474.

Ohgaki, R., N. Fukura, M. Matsushita, K. Mitsui, and H. Kanazawa. 2008. "Cell surface levels of organellar Na+/H+ exchanger isoform 6 are regulated by interaction with RACK1." *J Biol Chem* 283 (7):4417-29. doi: 10.1074/jbc.M705146200.

Olesen, C. W., J. Vogensen, I. Axholm, M. Severin, J. Schnipper, I. S. Pedersen, J. H. von Stemann, J. M. Schrøder, D. P. Christensen, and S. F. Pedersen. 2018. "Trafficking, localization and degradation of the Na." *Sci Rep* 8 (1):7435. doi: 10.1038/s41598-018-25059-7.

Onishi, I., P. J. Lin, G. H. Diering, W. P. Williams, and M. Numata. 2007. "RACK1 associates with NHE5 in focal adhesions and positively regulates the transporter activity." *Cell Signal* 19 (1):194-203. doi: 10.1016/j.cellsig.2006.06.011.

Parent, A., G. Laroche, E. Hamelin, and J. L. Parent. 2008. "RACK1 regulates the cell surface expression of the G protein-coupled receptor for thromboxane A(2)." *Traffic* 9 (3):394-407. doi: 10.1111/j.1600-0854.2007.00692.x.

Park, S. Y., and X. Guo. 2014. "Adaptor protein complexes and intracellular transport." *Biosci Rep* 34 (4). doi: 10.1042/BSR20140069.

Parker, M. D., and W. F. Boron. 2013. "The divergence, actions, roles, and relatives of sodium-coupled bicarbonate transporters." *Physiol Rev* 93 (2):803-959. doi: 10.1152/physrev.00023.2012.

Pierre, S., and K. Scholich. 2010. "Toponomics: studying protein-protein interactions and protein networks in intact tissue." *Mol Biosyst* 6 (4):641-7. doi: 10.1039/b910653g.

Praetorius, J., Y. H. Kim, E. V. Bouzinova, S. Frische, A. Rojek, C. Aalkjaer, and S. Nielsen. 2004. "NBCn1 is a basolateral Na+-HCO3- cotransporter in rat kidney inner medullary collecting ducts." *Am J Physiol Renal Physiol* 286 (5):F903-12. doi: 10.1152/ajprenal.00437.2002.

Praetorius, J., and S. Nielsen. 2006. "Distribution of sodium transporters and aquaporin-1 in the human choroid plexus." *Am J Physiol Cell Physiol* 291 (1):C59-67. doi: 10.1152/ajpcell.00433.2005.

Saras, J., and C. H. Heldin. 1996. "PDZ domains bind carboxy-terminal sequences of target proteins." *Trends Biochem Sci* 21 (12):455-8.

Seaman, M. N., A. Gautreau, and D. D. Billadeau. 2013. "Retromer-mediated endosomal protein sorting: all WASHed up!" *Trends Cell Biol* 23 (11):522-8. doi: 10.1016/j.tcb.2013.04.010.

Sedlyarov, V., R. Eichner, E. Girardi, P. Essletzbichler, U. Goldmann, P. Nunes-Hasler, I. Srndic, A. Moskovskich, L. X. Heinz, F. Kartnig, J. W. Bigenzahn, M. Rebsamen, P. Kovarik, N. Demaurex, and G. Superti-Furga. 2018. "The Bicarbonate Transporter SLC4A7 Plays a Key Role in Macrophage Phagosome Acidification." *Cell Host Microbe*. doi: 10.1016/j.chom.2018.04.013.

Simmen, T., S. Höning, A. Icking, R. Tikkanen, and W. Hunziker. 2002. "AP-4 binds basolateral signals and participates in basolateral sorting in epithelial MDCK cells." *Nat Cell Biol* 4 (2):154-9. doi: 10.1038/ncb745.

Stoops, E. H., G. A. Farr, M. Hull, and M. J. Caplan. 2014. "SNAP-tag to monitor trafficking of membrane proteins in polarized epithelial cells." *Methods Mol Biol* 1174:171-82. doi: 10.1007/978-1-4939-0944-5_11.

Swietach, P., R. D. Vaughan-Jones, A. L. Harris, and A. Hulikova. 2014. "The chemistry, physiology and pathology of pH in cancer." *Philos Trans R Soc Lond B Biol Sci* 369 (1638):20130099. doi: 10.1098/rstb.2013.0099.

Tanentzapf, G., and U. Tepass. 2003. "Interactions between the crumbs, lethal giant larvae and bazooka pathways in epithelial polarization." *Nat Cell Biol* 5 (1):46-52. doi: 10.1038/ncb896.

Traub, L. M. 2009. "Clathrin couture: fashioning distinctive membrane coats at the cell surface." *PLoS Biol* 7 (9):e1000192. doi: 10.1371/journal.pbio.1000192.

White, K. A., B. K. Grillo-Hill, and D. L. Barber. 2017. "Cancer cell behaviors mediated by dysregulated pH dynamics at a glance." *J Cell Sci* 130 (4):663-669. doi: 10.1242/jcs.195297.

Wu, B., and W. Guo. 2015. "The Exocyst at a Glance." *J Cell Sci* 128 (16):2957-64. doi: 10.1242/jcs.156398.